

Title of report:

Comprehensive Final Report for CDFA Agreement Number 17-0332-000-SA

Title of project:

The epidemiology of novel *PdR1* resistant grapevines: epidemic and vector movement models to support integrated disease management

Authors

Rodrigo P. P. Almeida
Dept. Environmental Science, Policy,
and Management
UC Berkeley
Email: rodrigoalmeida@berkeley.edu
Project Leader

M. Andrew Walker
Dept. Viticulture and Enology
UC Davis
Email: awalker@ucdavis.edu
Cooperator

Matt Daugherty
Dept. Entomology
UC Riverside
Email: mattd@ucr.edu
Cooperator

Perry de Valpine
Dept. Environmental Science, Policy,
and Management
UC Berkeley
Email: pdevalpine@berkeley.edu
Cooperator

Adam Kleczkowski
Dept. Computing Science and
Mathematics
University of Strathclyde
Glasgow, Scotland
Email: a.kleczkowski@strath.ac.uk
Cooperator

Time period covered by report

July 2017 to June 2019.

Layperson summary of project accomplishments

Resistant cultivars of agricultural crops are integral to sustainable integrated disease management strategies. Our previous work indicated that grapevines that express the *PdR1* gene exhibit resistance against *Xylella fastidiosa*, and are likely to slow the spread of *X. fastidiosa* among vineyards. In the current project, we have tested the generality of our previous observations, by testing *PdR1* resistant and susceptible genotypes into our vector transmission experiments and integrating greater biological detail into our epidemic modeling work. Our results suggest that the *PdR1* gene may lengthen the incubation period, increasing *X. fastidiosa* transmission, but induced resistance conferred by the gene may ultimately reduce spread over the long-term. Vector feeding preference, host resistance, and transmission are clearly dynamic, changing over the course of disease progression. It also remains unclear how growers may incorporate these hybrid plants into their production; we found that the longer the planned age of a vineyard, the greater the area that growers should plant with *PdR1* vines.

List of objectives

Specifically, we ask, under what ecological conditions and spatial arrangements will the use of *PdR1* vines reduce *X. fastidiosa* spread and maximize economic benefits to growers? The research consists of three objectives:

1. *Test the effects of PdR1 resistant plants on vector feeding preference and transmission of X. fastidiosa*
2. *Model the optimal mixture of PdR1 and susceptible grapevines to reduce X. fastidiosa spread and maximize economic return*
3. *Estimate dispersal of insect vectors from field population data*

Relevance statement

Development of grape cultivars resistant to *Xylella fastidiosa* is critical for effective and durable management of Pierce's disease. However, some forms of plant defense may enhance the risk of an epidemic. Our results confirm previous work in that *PdRI* resistant plants exhibit partial resistance to *X. fastidiosa*, resulting in reduced bacterial populations and reduced PD symptom severity. However, because *X. fastidiosa* is able to reach moderate population sizes in resistant plants, there is still significant vector transmission from these plants. Importantly, because of reduced symptom severity and vector feeding preference for healthy grapevines, transmission from resistant plants can be greater under some conditions. These results suggest that there may be a window of time where *PdRI* grapevines could act as reservoir hosts, amplifying vector transmission.

A critical question remains, under what ecological conditions, and for how long, could *PdRI* vines amplify transmission? We are working to address this question through epidemiological modeling. We also are working to describe conditions under which different mixtures of *PdRI* resistant and susceptible grapevines would maximize economic return for growers. Our bioeconomic modeling work suggests that a mixture of grapevines, with relatively more *PdRI* than susceptible would be optimal when 1) long-distance dispersal (but still within a vineyard) occurs and 2) when growers are interested in maximizing long-term gain. Overall, while there is some concern that *PdRI* vines could enhance *X. fastidiosa* spread in the field, our results suggest that these partially resistant vines hold promise to greatly improve Pierce's disease management. The key question remains to develop strategies to optimize their use in vineyards under a variety of realistic conditions.

Produced and pending publications

- Zeilinger, A.R., C. Wallis, D. Beal, A. Sicard, M. A. Walker, R.P.P. Almeida. Non-linear dynamics of vector transmission of a plant pathogen mediated by resistance cultivar and vector feeding preference. *Ecology*. In preparation.
- Zeilinger, A.R., D. Beal, A. Sicard, M.P. Daugherty, M.A. Walker, R.P.P. Almeida. Host defense and vector preference drive non-linear transmission dynamics for a plant pathogen. Bay Area Ecology and Evolution of Infectious Disease, Stanford University, Palo Alto, CA. 2 March 2019.
- Almeida, R.P.P. 2019. Ecology of the 'other' vector-borne plant diseases: similar questions and challenges? International Plant Virus Epidemiology Conference; Seoul, South Korea.
- Zeilinger, A.R., M. Daugherty, C. Del Cid, R. Krugner, R.P.P. Almeida. 2018. Influence of climate change on vector-borne pathogen spread: Improving management of *Xylella fastidiosa* in uncertain times. Annual Meeting of the Entomological Society of America. Vancouver, BC, Canada. 11 November 2018.
- Almeida, R.P.P. 2018. Australasian Plant Pathology meeting at New Zealand Plant and Food Research - Biosecurity workshop. Led afternoon discussion on risks associated with *X. fastidiosa*.
- Almeida, R.P.P. 2018. Evaluating potential shifts in PD epidemiology. California Department of Food and Agriculture, Sacramento CA. CDFA Nursery Board.
- Almeida, R.P.P. 2018. The emerging threat of *Xylella fastidiosa* to European viticulture. International Congress on Grapevine and Wine Sciences. Logrono, Spain.
- Zeilinger, A.R., D. Beal, A. Sicard, M.P. Daugherty, M.A. Walker, R.P.P. Almeida 2017. Fear your tolerant neighbors: assessing epidemic risks from novel plant defenses against a vector-borne pathogen of grapevines. Ecological Society of America Meeting, Portland, OR. August 2017.
- Almeida, R.P.P. 2017. *Xylella fastidiosa*: new risks from an old threat. European Conference on *Xylella fastidiosa*: finding answers to a global problem. Palma de Mallorca, Spain.

Status of funds

Funds were used as originally proposed.

Summary of IP
Not applicable.

Abstract

Host resistance against vector-borne plant pathogens is a critical component of integrated disease management. However, theory predicts that traits that confer tolerance or partial resistance can, under some ecological conditions, enhance the spread of pathogens and spillover to more susceptible populations or cultivars. The host selection behavior of vectors based on infection status appears to be key in driving epidemic risk from tolerant hosts. At the same time, while recent theory has further emphasized the importance of infection-induced host selection behavior by insect vectors for plant disease epidemiology, experimental tests on the relationship between vector feeding preference and transmission are lacking. Such tests are critical to inform future developments of theory. Here we test how vector feeding preference mediates transmission from hybrid grapevine cultivars providing defense against the pathogenic bacterium *Xylella fastidiosa*, conferred by the *PdRI* gene. We measure a range of epidemiologically relevant parameters in a series of vector transmission experiments and show that 1) vector feeding preference changes over the course of disease progression, 2) vector feeding preference is clearly important but does not predict transmission alone, and 3) the duration of the incubation period, in which plant hosts are infectious but asymptomatic, is likely when most vector transmission occurs. Our results suggest, consistent with theory, that the *PdRI* gene may lengthen the incubation period, increasing *X. fastidiosa* transmission, but induced resistance conferred by the gene may ultimately reduce spread over the long-term. Vector feeding preference, host resistance, and transmission are clearly dynamic, changing over the course of disease progression, in *X. fastidiosa* pathosystems and likely other systems. Understanding these dynamics is critical for broader insights into the epidemiology of vector-borne plant pathogens. Below we present a detailed report of work done in this project.

Introduction

Host defense against pathogens is critical for determining disease epidemics broadly. Defense against pathogens in agricultural crops is one of the most successful and durable strategies to manage agricultural diseases (Power 1990; Mundt 2002; Gilligan 2008). Defense against pathogens can be broadly categorized as either resistance or tolerance. Resistance alleviates the fitness costs of infection by reducing the pathogen population in host tissues; tolerance alleviates the fitness costs by ameliorating disease symptoms with little effect on pathogen population size (Boots 2008). Variation among hosts in tolerance and resistance can be maintained over evolutionary timescales through ecological feedbacks (Best et al. 2008), and has important epidemiological consequences (Dwyer et al. 1997; Lloyd-Smith et al. 2005; Boots 2008; Laine et al. 2011; Borer et al. 2016). Generally, tolerance traits are expected to increase the prevalence of a pathogen within a host population (Roy and Kirchner 2000; Miller et al. 2006; Best et al. 2008; Zeilinger and Daugherty 2014).

While variation in host defense may play an important role in vector-borne pathogen spread—as seen broadly with directly transmitted pathogens—this question has received relatively little attention in the literature. Moreover, we might expect the relationships between defense and vector transmission to be distinct from that of directly transmitted pathogens because of the complexity of vector transmission and host selection (Zeilinger and Daugherty 2014; Sisterson and Stenger 2018). A recent flourishing of theory on plant disease epidemiology has sought to describe the range of influences that host selection by vectors may have on pathogen spread. Much of this work is focused on vector feeding preferences dependent on infection status of host as well as infection status of the vector itself.

Early models showed that vector preference conditional on infection status could enhance spread of pathogens during early stages of an epidemic (Kingsolver 1987; McElhany et al. 1995). More recent models have provided greater nuance by distinguishing effects of behaviors around attraction/settling vs. leaving/departure of vectors (Sisterson 2008; Shaw et al. 2017; Donnelly et al. 2019), combining effects of preference conditional on infection status of the vector as well as of the host (Roosien et al. 2013; Shaw et al. 2017; Donnelly et al. 2019), exploring the implications for different modes of transmission—whether characterized as persistent or non-persistent transmission (Shaw et al. 2017; Donnelly et al. 2019), and exploring the intersection of vector preference and multi-species host communities on spread (Shoemaker et al. 2019).

Vector feeding preference conditional on infection status of hosts or of the vector itself, i.e., “infection-induced vector preference”, has been documented empirically in numerous plant disease systems, including those caused by fungal, bacterial, and viral pathogens (reviewed by Eigenbrode et al. 2018). The above mentioned modeling work has emphasized the importance of infection-induced vector preference on transmission and spread. Specifically, Shaw et al. (2017) used a sensitivity analysis of their model to predict that components of vector preference had less impact on pathogen spread than life history traits, but that spread remained sensitive to infection-dependent leaving and attraction rates of vectors. However, few empirical studies have attempted to measure the role that preference plays in transmission. And thus the widespread theoretical predictions on the influence of vector preference on pathogen spread remain largely untested. Furthermore, the dominant hypotheses describing how infection-induced vector preference arises from evolutionary processes—the host and vector manipulation hypotheses (Gandon 2018), similarly rely on untested theory linking vector behavior to pathogen spread and, in turn, pathogen fitness.

A central challenge in measuring the relationship between vector behavior/manipulation and transmission is experimentally inducing variation in vector host choice and transmission concurrently. Del Cid et al. (2018) qualitatively considered vector transmission of *X. fastidiosa* between a “choice” experiment in which vectors were free to choose between an infected source grapevine and a healthy test plant vs. a “no choice” experiment in which vectors were sequentially confined to an infected plant then a healthy plant. The authors found striking differences in the transmission rates between these scenarios, suggesting that vector choice played an important role. However, preference or movement was not measured in the experiments, undermining any robust interpretations. Alternatively, some studies have shown that vector host selection varies dynamically as disease progresses (Blua and Perring 1992; Werner et al. 2009; De Moraes et al. 2014; Daugherty et al. 2017). However, the only study to our knowledge that showed an empirical relationship between vector preference and transmission was conducted by Daugherty et al. (2017), which showed that increasing vector avoidance of *X. fastidiosa*-infected grapevines as disease progressed coincided with reduced transmission to healthy host plants over different temperature regimes.

Comparing vector preference and transmission among plant species or genotypes varying in levels and forms of defense could also offer a means to test for preference-transmission relationships. Tolerant hosts decouple the phenotypic responses of infection—which are often used by vectors in host selection (Eigenbrode et al. 2018)—from pathogen burden and therefore allow for a decoupling of the influences of preference and pathogen population size on transmission. Furthermore, as hypothesized by Zeilinger and Daugherty (2014), the interactions between different forms of defense and vector preference can have important epidemiological implications: traits conferring resistance against a pathogen should broadly reduce pathogen spread regardless of the particularities of vector preference; however, pathogen spread can be greatly enhanced when hosts are tolerant to infection *and* vectors avoid diseased hosts; in such cases tolerant hosts can act as effective reservoirs. The precise interplay between host defense and vector transmission are critical for effective disease management because of the risk of disease spillover from partially resistant or tolerant hosts into nearby susceptible host populations (Sisterson and Stenger 2018) as well as the durability of defensive traits against the evolution of pathogens (Watkinson-Powell et al. 2019).

Xylella fastidiosa (family Xanthomonadaceae) is a xylem-limited bacterial plant pathogen and causes diseases in many crop species, including Olive Quick Decline Syndrome, Citrus Variegated Chlorosis, Pierce’s disease of grapevines, and leaf scorch of almond, oleander, and coffee (Sicard et al. 2018). As suggested by the broad list of diseases, *X. fastidiosa* is an extreme generalist, associated with at least 350 botanical taxa (EFSA Panel on Plant Health 2015). *Xylella fastidiosa* is transmitted in a propagative persistent but non-circulative manner by xylem-feeding insect vectors in the family Cicadellidae and superfamily Cercopoidea, with all xylem-feeding Hemiptera regarded as potential vectors (Sicard et al. 2018). To date, the infection-induced host selection behavior of five cicadellid vectors have been studied and all have shown avoidance of *X. fastidiosa*-infected symptomatic plant hosts but no discrimination between infected asymptomatic hosts and uninfected (Marucci et al. 2005;

Daugherty et al. 2011; De Miranda et al. 2013). Orientation through visual cues probably underlies this preference (Daugherty et al. 2011). The potential effects of vector infection status on preference has not been studied.

Pierce's disease of grapevines has led to widespread losses in agricultural production in California viticulture (~\$100 million per year, Tumber et al. 2014). Furthermore, insecticide use to manage vectors of *X. fastidiosa* potentially harms biodiversity and provisioning of agroecosystem services (Daugherty et al. 2015). Alternatively, California vineyard managers have shown a strong interest in using resistant grapevines to manage Pierce's disease (Zeilinger *unpublished data*). Recently, hybrids between domesticated grape *Vitis vinifera* and North American native congener *V. arizonica*, have shown promising levels of resistance against *X. fastidiosa* (Krivanek et al. 2006). Resistance is conferred by the *PdR1* dominant locus, and while the precise mechanism of resistance is still unresolved, backcrossed lines harbor much lower populations of *X. fastidiosa* and exhibit negligible disease symptoms (Krivanek and Walker 2005). Interestingly, *V. arizonica* is native to southwestern United States and northern Mexico, where *X. fastidiosa* is endemic and where cultivation of susceptible grapevines is nearly impossible due to high disease pressure, although there are reasons that *PdR1* resistance arose through coevolution with *X. fastidiosa* (Riaz et al. 2018).

Based on current evidence, *PdR1* hybrid grapevines are best characterized as being partially resistant; *X. fastidiosa* population sizes are 4 – 5 orders of magnitude lower in *PdR1* vines than susceptible grapevines, population size can still far exceed that required for vector transmission (Hill and Purcell 1997; Krivanek and Walker 2005). Given that symptom development is very slow (Krivanek et al. 2005) and insect vectors avoid diseased plants, there is significant risk that *PdR1* grapevines could act as reservoir hosts of *X. fastidiosa*, enhancing vector transmission among vines and spillover to more susceptible vineyards (Zeilinger and Daugherty 2014; Sisterson and Stenger 2018). Specifically, we hypothesize that transmission from tolerant hosts could exceed that from susceptible hosts when increasingly severe disease symptoms lead to vector avoidance and lower acquisition (Fig. 1).

We aimed to assess the risk of enhanced transmission by the efficient cicadellid vector *Graphocephala atropunctata* from inoculated *PdR1* resistant grapevines and closely related susceptible vines through a combined preference-transmission experiment. We compared Pierce's disease symptom severity, *X. fastidiosa* population size, vector attraction and leaving rates, vector acquisition rates, and vector transmission rates from *PdR1* resistant and susceptible vines over multiple points of disease progression. We fit a series of non-linear models to transmission curves to test our hypothesis on the risk of enhanced transmission from *PdR1* vines. Finally, we employed a machine learning approach—the elastic net algorithm—to test which set of transmission parameters best explained variation in transmission. From this we provide the best empirical test to date of the relationship between components of infection-induced vector preference and transmission.

Materials and Methods

Objective 1. Test the effects of PdR1 resistant plants on vector feeding preference and transmission of X. fastidiosa

Plants and Insects

All resistant and susceptible genotypes were segregants of a cross between *Vitis vinifera* cv. Airen and a hybrid of *V. rupestris* x *V. arizonica* (b40-14 background), with resistance conferred by the *PdR1c* gene (Krivanek et al. 2006; Walker and Tenschler 2016). We repeated the transmission experiment over two years: in 2016, the Resistant genotype was line 07744-006 and the Susceptible genotype was line 07744-007; in 2017, we used two Resistant genotypes, 07744-094 and 07744-102, and two Susceptible genotypes, 07744-007 and 07744-092. For simplicity in any discussion of genotypes in the 2017 experiment, below, we abbreviate with the last three digits: indicating the Resistant genotypes as 094 and 102, and the Susceptible genotypes as 007 and 092.

In both years, transmission trials were conducted with green cuttings made from Resistant and Susceptible genotype plants; we grew the cuttings in 1-gal pots with a 5:1:1 mixture of Supersoil (Rod McLellan Company, San Mateo, CA, USA), perlite, and sand in a greenhouse at the Oxford Tract, UC

Berkeley (average temperature 23.5°C, with ambient daylight). We added 1 tsp of Osmocote Plus fertilizer (N-P-K 15-9-12) about two months after planting. We watered the grapevines every 2 days and treated with fungicides for powdery mildew control as needed (at most every 2 weeks) with a rotating schedule of wettable sulfur (Sulfur DF*), potassium bicarbonate (Kaligreen*), trifloxystrobin (Compass O*), myclobutanil (Eagle*), and thiophanate-methyl (3336*) at label rates.

To establish *X. fastidiosa*-infected plants, in May of both years, we needle inoculated 3-month-old Resistant and Susceptible vines near the base of the main stem with 10 µl of a turbid suspension ($OD_{600} > 1$) of *X. fastidiosa* culture (STL isolate, originally isolated from a symptomatic grapevine in Napa Valley, CA, USA) in SCP buffer as described in Hill and Purcell (1995). In 2016, we needle inoculated two points with 5 µl; in 2017, we needle inoculated just one point with 10 µl. Test plants were mock-inoculated with 10 µl of SCP buffer only.

Colonies of *Graphocephala atropunctata* (Signoret) (blue-green sharpshooter, Hemiptera: Cicadellidae) were started from individuals collected from wild grape (*Vitis californica* Benth), Himalayan blackberry (*Rubus armenicus* Focke), and common nettle (*Urtica dioica* L.) from Sonoma and Alameda counties, California, USA, in April and May, and in Humboldt county, CA, in June and July. We reared *G. atropunctata* on basil (*Ocimum basilicum* L.) changed weekly. Prior to transmission trials, we pre-screened all insects for *X. fastidiosa* infection by placing groups of 10 insects on greenhouse-grown grapevines (cv. Cabernet Franc, certified free of *X. fastidiosa* infection by Foundational Plant Services, UC Davis) for 5-7 days. Plants were cultured 12 weeks later; all were free of *X. fastidiosa* infection in 2016 whereas in 2017 three trials were removed from analysis because of vector infectiousness prior to the trials.

Transmission experiment

In both years, we paired one *X. fastidiosa*-free test plant of the Susceptible genotype and one inoculated source plant—either Resistant or Susceptible—in a BugDorm tent-style cage (61 cm³, BioQuip Products, Inc., Rancho Dominguez, CA, USA). Each plant was trimmed to a single stem and six main-stem leaves one week prior to the trials. We paired Resistant genotype 094 source plants with Susceptible genotype 092 test plants and Resistant genotype 102 source plants with Susceptible genotype 007 test plants; for Susceptible source plants the test plant was of the same genotype. At the beginning of the trials, eight adult BGSS were introduced into each cage between 10:00 and 12:00 in the morning. Prior to introducing the insects, we chilled them for two minutes in a -20°C freezer to prevent them from escaping or dispersing immediately to a plant; we then introduced them in the middle of the cage, equidistant from the two plants. In 2016, we repeated the trials at 3 weeks, 8 weeks, and 12 weeks post-inoculation. In 2017, we repeated the trials at 2, 5, 8, and 14 weeks post-inoculation. Additionally, due to the large number trials run in 2017, we ran the replicates in two temporal blocks, two weeks apart and using a randomized complete block design. Each combination of genotype and weeks post-inoculation was replicated 8 times in both years.

Once the BGSS were introduced to the cage, we recorded the number of insects on each plant and in neutral space (cage walls and pots) repeatedly at pre-determined times from the start of the trials. In 2016, these times were: 1 min, 5 min, 10 min, 15 min, 30 min, 45 min, 1 hr, 2 hr, 4 hr, 6 hr, 24 hr, 30 hr, 48 hr, 3 d, 4 d, 5 d, 6 d, 7d, and 8 d. In 2017, we used the same time points but shortened the total duration of the trials to 4 d, because the 2016 data showed that the BGSS reached equilibrium in their movements by 4 d and this should reduce mortality during the trials. In 2016, 7% of insects died in our trials (27 out of 384 total); in 2017, 10% of insects died (107/1024).

Ancillary studies on induced resistance

In 2016 we saw evidence of induced resistance in *PdRI* Resistant plants at after eight weeks post-inoculation as a strong decline in *X. fastidiosa* populations and vector transmission (see *Results* below). In 2017 we investigated this with two ancillary studies.

First, we measured a wide profile of secondary metabolites from inoculated source plants within our transmission experiment. At the end of each trial, we collected two leaf blades and a 3 cm section of

woody stem from each *X. fastidiosa*-infected source plant. Each sample was immediately frozen in liquid nitrogen and then stored at -20°C until chemical analysis. We collected samples only from genotypes 092 Susceptible and 094 Resistant for logistical reasons.

Second, we conducted a re-infection experiment. In June 2017, we needle inoculated a set of plants using the same four genotypes as described above. But here we repeatedly measured population size of *X. fastidiosa* in petioles using serial dilution at 3, 9, and 16 weeks post-inoculation. We then inoculated a random subset of these plants a second time at 17 weeks post-inoculation, and inoculated an additional set of plants that were free of *X. fastidiosa*. This produced three treatments: 1) plants inoculated once in June; 2) plants inoculated once in October; and 3) plants inoculated twice. We then estimated *X. fastidiosa* population size from all plants at 21 and 26 weeks post-inoculation (from the first inoculation date). Sample size for each treatment-genotype combination was four plants.

Bacterial culturing and qPCR

At the end of the trials, we removed all insects and noted the severity of Pierce's disease symptoms on the source plants using the 0 – 5 symptom scoring index developed by Guilhabert and Kirkpatrick (2005). Within three days after the trials finished, we estimated *X. fastidiosa* populations in the source plants by serial culturing of three petioles, and twelve weeks later we assayed the infection status of all test plants (Hill and Purcell 1995). At the end of the trials, insects were frozen at -80°C until we assayed them for *X. fastidiosa* infection status using qPCR. We extracted DNA from *G. atropunctata* heads using the Qiagen DNEasy Blood and Tissue kit (Hilden, Germany) as described in (Daugherty et al. 2009). Our *X. fastidiosa* DNA target fragment was amplified on a 7500 real-time thermocycler (Applied Biosystems, Foster City, CA) using SYBR Green fluorophore and the PD0059 F+R primers designed by Sicard et al. (*in review*). We then estimated corrected baseline fluorescence and amplification efficiency using the algorithms described in Ruijter et al. (2009).

Statistical analysis

We first tested for differences in transmission-associated variables among genotypes, weeks post-inoculation, and interaction between genotype and weeks post-inoculation, resulting in ANCOVA linear models. In 2017, we included a block main effect but analyses were otherwise identical between 2016 and 2017 experiments. We first tested for differences in Pierce's disease symptom severity in source plants with a partial odds ordinal logistic regression model, because the response variable—PD symptom index—represented an ordinal categorical variable (Harrell 2015). We analyzed variation in population size of *X. fastidiosa* in inoculated source plants using a generalized linear model with quasi-Poisson distributed error to correct for over-dispersion. While the quasi-Poisson model showed modest non-constant error variance, it performed much better than Poisson or negative binomial regression models (*results not shown*).

We sought to test for preference of *G. atropunctata* vectors for *X. fastidiosa*-infected source plants or *X. fastidiosa*-free test plants by estimating attraction and leaving rates from the two plants. Zeilinger et al. (2014) developed a mechanistic bio-statistical model on movement of a single consumer between two simultaneous choices; Gray et al. (*in review*) then generalized this model for multiple consumers within a preference trial. We fit our repeated measures count data on *G. atropunctata* location to the generalized model of Gray et al. (*in review*) for each combination of plant genotype and weeks post-inoculation. We fit four model variants—representing null and alternative hypotheses on differences and mechanisms of preference—and selected the best set of models based on Akaike's Information Criterion corrected for small sample size (AIC_c), as described in (Supplementary Information, Appendix A). We calculated 95% confidence intervals using the quadratic approximation method (Bolker 2008) and used multi-model averaging of all models with $\Delta AIC_c \leq 7$ (Burnham et al. 2011). This resulted in robust estimates and uncertainty for attraction rates and leaving rates from each source plant and test plant for each combination of plant genotype and weeks post-inoculation. See Supplementary Information, Appendix A for additional information on testing assumptions of the consumer movement model.

For the analysis of vector acquisition and transmission of *X. fastidiosa*, we expected *a priori* potential non-linear dynamics. As such we fit a series of non-linear models, including two unimodal models, Holling Type IV and Ricker models, and two saturating or asymptotic models, Michaelis-Menten and Logistic Growth models, as well as a linear model as a “null hypothesis” (Supplementary Information Appendix B). Based on the best fitting model, we compared 95% confidence intervals of parameter estimates to infer if dynamics clearly differed between Resistant and Susceptible genotypes.

We investigated which set of explanatory variables—measured from our experiments—best explained variation in infection status of test plants (i.e., vector transmission). For explanatory variables, we included resistance trait (i.e., whether source plant was Resistant or Susceptible), proportion of vectors infectious with *X. fastidiosa*, population size of *X. fastidiosa* in source plant, disease severity index, attraction rate toward source plant, attraction rate toward test plant, leaving rate from source plant, leaving rate from test plant. The attraction and leaving rates were estimated for each trial using the Consumer Movement Model described earlier. We did not include weeks post-inoculation because our results of transmission dynamics indicate strong linearities between transmission over time. The best set of linear predictors with infection status was determined using the elastic net algorithm (Zou and Hastie 2005). The elastic net combines the penalties of ridge regression and LASSO (Least Absolute Shrinkage and Selection Operator) algorithms. As such it is particularly well-suited for variable selection (i.e., shrinking coefficient estimates toward zero) when explanatory variables co-vary (James et al. 2013), which we expected *a priori* since the explanatory variables are all inter-related to the transmission process and because of the prevalence of correlations among attraction and leaving rates estimated from the CMM. Elastic net requires “tuning” two regularization parameters, α and λ , for which we used repeated k-fold cross-validation. We chose $k = 5$, chose the best parameter values by maximizing the area under the curve of the Receiver Operating Characteristic (ROC), and ran cross-validation 500 times to estimate a mean and SD for each coefficient estimate. We assumed that the response variable—infection status of the test plant—was binomially distributed.

We first analyzed data on plant secondary metabolites by examining broad differences using a multivariate ANOVA (MANOVA). The response variables were total phenolics in leaf blades, total phenolics in stems, and volatiles in leaf blades (the analysis of volatiles in stems could not be completed due to lack of tissue); the explanatory variables were resistance status (genotype 092 Susceptible vs. genotype 094 Resistant), weeks post-inoculation, and the interaction between the two. We report differences with Pillai’s trace, though Wilks’ λ , Hotelling’s trace, and Roy’s greatest root produced equivalent results (Johnson and Field 1993). Second, we explored differences between genotypes, and how these differences change over time, using principal components analysis of all 105 secondary metabolites isolated from our samples (Supplementary Material, Appendix C). Third, we investigated what set of secondary metabolites best explained variation in attraction and leaving rates of *G. atropunctata* to and from infected source plants using elastic net. In employing elastic net, we sought to find the best set of compounds that explained vector feeding behavior, similar to principal components regression (Pareja et al. 2009). Principal components regression and ridge regression—a special case of elastic net—produce similar results given that the first few principal components capture most variation in the data set (James et al. 2013). However, principal components regression does not naturally allow for selecting a subset of parameters; elastic net allows for such parameter or model selection through shrinking some coefficients to zero (James et al. 2013).

For the reinfection experiment, if Resistant plants exhibited stronger induced resistance, we hypothesized that we would see the greatest decline in population size of *X. fastidiosa* in Resistant plants that had been previously inoculated. As such, we focused our analysis on 21 and 26 weeks post-inoculation and only for the two treatments inoculated in October. We tested for divergent slopes in *X. fastidiosa* population size between treatments and resistance trait; because of low sample size, we combined genotypes based on presence of resistance trait. We adopted an ANCOVA-style model because we were specifically interested in the three-way interaction between week, treatment, and resistance trait. We used a generalized linear model with negative binomial error distribution because the *X. fastidiosa* population data were over-dispersed.

All analyses were performed in R 3.5.3 (R Core Team 2019). To fit consumer movement models, we used the `optimx` package with the Spectral Gradient optimization algorithm (Nash and Varadhan 2011); to fit non-linear transmission models and perform model selection with AIC_c , we used the `bbmle` package (Bolker and R Core Team 2017). We used the `rms` package to perform partial odds ordinal logistic regression on Pierce’s disease symptom severity (Harrell 2019). For the elastic net algorithm in the analysis of defensive phytochemistry and transmission, we used the `glmnet` package and cross-validated the tuning parameters using the `caret` package (Friedman et al. 2010; Kuhn et al. 2018). For the negative binomial GLM, we used the `MASS` package (Venables and Ripley 2002).

2. Model the optimal mixture of PdR1 and susceptible grapevines to reduce *X. fastidiosa* spread and maximize economic return

We built an economic extension to our vector-SI epidemic model, described in our proposal. We consider a scenario where two vineyards are grown adjacent to each other—one composed of a grape cultivar susceptible to Pierce’s Disease, Patch 1, and another composed of *PdR1* resistant grapevines, Patch 2. For the economic model, we followed the framework of Macpherson et al. (2017) and assumed that yield is proportional to the density of healthy or asymptomatic hosts at harvest time, t .

In our previous analyses of the bioeconomic model, we assumed that transmission was frequency-dependent. However, after extensive research into the literature and model exploration, we adopted a density-dependent form of transmission here. Density-dependent transmission is generally thought to relate to pathogen systems where the pathogen spread beyond the immediate neighbors of an infected host is relatively common. As vector-borne pathogens often exhibit more frequent long-distance dispersals, adopting a density-dependent transmission term seems reasonable. Our model then takes the form:

$$H(\delta) = \delta L(1 - R_p) + I_A(t, \delta) + I_B(t, \delta)$$

$$\frac{dI_A}{dt} = \beta_A ((1 - \delta)L - I_A(t, \delta))(I_A(t, \delta) + \mu I_B(t, \delta) + \varepsilon)$$

$$\frac{dI_B}{dt} = \beta_B (\delta L - I_B(t, \delta))(I_B(t, \delta) + \mu I_A(t, \delta) + \varepsilon)$$

Here, $H(\delta)$ represents monetary loss after harvest, as a function of the proportion of area planted to *PdR1* vines, δL , the value of *PdR1* grapes relative to susceptible grapes, $(1 - R_p)$, the density of diseased susceptible vines $I_A(t, \delta)$ and the density of diseased *PdR1* vines $I_B(t, \delta)$. These last two terms are then modeled dynamically and using density-dependent transmission. The within-patch transmission rate, β , differs between grape genotypes while we assume that cross-patch transmission, μ , and primary infection, ε , are equal between genotypes.

3. Estimate dispersal of insect vectors from field population data

We expanded our original vision of the vector dispersal models, and focusing our efforts on modeling the spread of *X. fastidiosa*. We are using data collected by our research group and colleagues of disease surveys and BGSS abundance in ~30 commercial vineyard sites across Napa and Sonoma from 2016 – 2018. We are currently working to fit a spatiotemporal stochastic epidemic model developed by Drakey et al. (2017) to our Pierce’s disease survey data:

$$\lambda_i(t) = \left(\beta \sum_{j \in I(t)} K(d_{ij}, \alpha) \right)$$

$$K(d, \alpha) = \frac{1}{1 + \beta d^\alpha}$$

where $\lambda_i(t)$ is the instantaneous force of infection on host i at time t , β is the vine-to-vine “contact rate” or rate of secondary spread, ε is the primary or external infection rate, and $K(d_{ij}, \alpha)$ is the dispersal kernel. The dispersal kernel is a function of distance between uninfected host i and infected host j and the dispersal parameter α . We assume that dispersal takes the functional form of a normalized exponential decay function, following Adrakey et al. (2017). However, the dispersal function could take different forms (Neri et al. 2014). Note that the summation, $\sum_{j \in I(t)} K(d_{ij}, \alpha)$, represents the dispersal from every infected host j to the uninfected host i at time t . The full likelihood function—in which the instantaneous force of infection is estimated for every uninfected host—is described in Adrakey et al. (2017).

We built a customized MCMC sampler and implemented it in the R computing environment using the nimble package for Bayesian modeling, whereas the original model was implemented in C++ (Adrakey et al. 2017). Implementing the MCMC sampler and model have required more extensive programming work than expected. However, the result will be a model that will be easier for additional researchers to use as it is implemented in the more widely used R computing environment. This work will be continued as part of our larger North Coast Pierce’s Disease project. We also plan to extend the model to explicitly incorporate vector dispersal in the model of pathogen dispersal. In any vector-borne disease system, pathogen dispersal should be a function of vector dispersal. From this work, we will be able to estimate vector dispersal directly from field data as well as the relationship between vector dispersal and pathogen spread. We will also be able to estimate the relative importance of vine-to-vine spread and primary infection rate, which Pierce’s disease scholars have been debating for some time.

Results

Pierce’s disease and X. fastidiosa population dynamics

In both years, inoculated Susceptible grapevines exhibited Pierce’s disease symptoms earlier and more severely than inoculated Resistant grapevines (Fig. 2a, b). In 2016, we could not detect a significant effect of week or difference in genotypes (week post-inoculation: estimate \pm SE = 2.692 \pm 6.885, Wald Z = 0.39, P = 0.696; week-by-genotype interaction: estimate \pm SE = 1.137 \pm 8.074, Z = 0.14, P = 0.888). In 2017, we found a clear trend of increasing symptom severity over time and a clear difference between Susceptible genotype 007 and Resistant genotype 102 (week: estimate \pm SE = 0.706 \pm 0.141, Z = 5.00, P < 0.0001; week-by-genotype interaction between 007 and 102: (estimate \pm SE = -0.463 \pm 0.183, Z = -2.53, P = 0.012).

Both Susceptible and Resistant vines harbored substantial populations of *X. fastidiosa* throughout our experiments, though populations in Resistant lines were consistently lower (Fig. 2c, d). In 2016, *X. fastidiosa* populations increased over time and were clearly greater in Susceptible compared to Resistant lines (week post-inoculation: estimate [95% confidence intervals] = 0.321 [0.0914, 0.660], t = 2.32; genotype: estimate [95% CI] = 2.96 [0.340, 6.94], t = 1.85). There was no clear interaction between weeks and genotype (estimate = -0.122 [-0.471, 0.128], t = -0.835). In 2017, we found no clear increase in *X. fastidiosa* populations over time (weeks: estimate = 0.0382 [-0.0262, 0.102], t = 1.18). However, *X. fastidiosa* populations were substantially lower in the Resistant genotypes than the Susceptible genotypes 007, which was used as a baseline (Resistant line 094: estimate = -1.91 [-3.71, -0.448], t = -2.34; Resistant line 102: estimate: -1.86 [-3.83, -0.293], t = -2.11).

Vector host selection

Over both years of our experiment, *G. atropunctata* showed little discrimination between host plants in early trials, i.e., two to five weeks post-inoculation (Fig. 3, Supplementary Information Appendix A Tables A3 and A4). In 2016, *G. atropunctata* showed no preference for either host plant except for in trials with the Susceptible genotype at 12 weeks post-inoculation (Fig. 3, Table A3). Here, vectors showed slightly greater attraction rates toward the test plant and slightly lower leaving rates from the test plant relative to the inoculated source plant. However, the 95% confidence intervals were quite large (Fig. 3).

In the 2017 experiments, differences in plant choice appeared earlier and showed greater differences. At two and five weeks post-inoculation, *G. atropunctata* showed a slight preference for test plants in trials with genotypes 092 Susceptible and 094 Resistant. In the other trials, they showed no preference, with the Fixed model being the best model to fit the data (Fig. 3, Table A4). At eight weeks post-inoculation, *G. atropunctata* showed greater attraction rates toward test plants relative to Resistant source plants (genotypes 094 and 102)—the difference being particularly significant with genotype 094 (Fig. 3). At 14 weeks post-inoculation, *G. atropunctata* showed strong preference for test plants relative to Susceptible source plants (genotypes 007 and 092), realized mostly through different attraction rates, though leaving rates were slightly different as well. While vectors showed similar preferences in trials with Resistant genotypes, the differences were not as clear (Fig. 3, Table A4).

Comparing across years, overall movement rates were not clearly greater in one year over the other. Attraction rates were on average greater in 2016 (2016 mean attraction rate = 0.713 hr^{-1} ; 2017 mean attraction rate = 0.633 hr^{-1}) but leaving rates were much greater in 2017 (2016 mean leaving rate = 0.0165 hr^{-1} ; 2017 mean leaving rate = 0.0673 hr^{-1}).

Vector acquisition and transmission

For the vector acquisition analysis, unimodal models performed the best in both years. In 2016, the Ricker model fit the data best for both the Susceptible and Resistant genotypes (Supplementary Information Appendix B, Table B2). Because the Ricker model was selected for both genotypes, we can make inferences based on parameter estimates and 95% CI. While vector acquisition was consistently greater from Susceptible grapevines, the parameter estimates did not differ based on 95% confidence intervals (Fig. 4a, Table B3). The b parameter of the Ricker model determines the timing of peak acquisition (Bolker 2008), with peak acquisition occurring slightly earlier in trials with Resistant plants ($1/b = 6.25$ weeks post inoculation) than in trials with Susceptible plants ($1/b = 6.58$ weeks).

In 2017, the Holling Type IV model fit the acquisition data best for both Susceptible and Resistant genotypes (Table B2). Here, vector acquisition was consistently greater from Susceptible than Resistant grapevines and—based on 95% CI of parameter estimates—was significantly so (Fig. 5b, Table B3). The peak of vector acquisition is predicted to be only slightly earlier for the Resistant lines ($-2b/c = 7.55$ weeks) than for the Susceptible lines ($-2b/c = 7.91$ weeks). At the same time, the long-term vector acquisition rate is predicted to be much lower from the Resistant lines ($a = 0.049$) than from the Susceptible lines ($a = 0.111$) (Table B3), reflecting the lower peak acquisition rate from Resistant lines (Fig. 5b). Comparing between years, vector acquisition was overall greater and peaked earlier in 2016 compared to 2017 (Figs. 5a and 5b).

For analysis of transmission to test plants, there was little overall clear separation among models, with AIC_c values being relatively similar (Supplementary Information Appendix B Table B4). In 2016, three models fit the data from the Resistant genotype equally well: the Logistic Growth, Ricker, and Linear models. However, examining the parameter estimates, the fits of the Logistic Growth and Linear models resulted in very high transmission rates at the y-intercept (i.e., at the start of the trials), which would be biologically implausible. In the end, we selected the Ricker model as it predicts a transmission rate near zero at the y-intercept. Likewise, the Logistic Growth, Ricker, and Linear models fit the data from the Susceptible genotype in 2016 similarly, though the Ricker model was slightly better. The a parameter determines the slope of the line near the origin, which is estimated to be much larger for the Resistant plants ($a = 0.704$) than for the Susceptible plants ($a = 0.399$) (Fig. 5c); however, the confidence

intervals for both estimates are large, making inferences difficult (Table B5). At the same time, confidence intervals of the b parameter estimates overlapped only slightly, suggesting a clearer difference in the time of peak transmission. Transmission from Resistant genotypes peaked earlier ($1/b = 2.9$ weeks post-inoculation) than transmission from Susceptible genotypes ($1/b = 5.1$ weeks) (Fig. 5c). Both curves suggest a similar probability of transmission rate at the peak (~ 0.75)

In 2017, transmission was overall slightly greater from Resistant plants (total proportion of test plants infected = 0.234) than from Susceptible plants (0.203), though transmission from Resistant plants was much more dynamic (Fig. 5d). Fitting non-linear models to data from Susceptible genotypes in 2017 resulted in the Ricker model being the best model, though Michaelis-Menten provided a similar fit (Table B4). In contrast, data from Resistant genotypes resulted in better separation among models, with the Holling Type IV model being selected as the best fit. Different models were selected as the best models, indicating qualitatively different dynamics for transmission from the Resistant and Susceptible genotypes. The low estimate of the a parameter (0.069) of Holling Type IV suggests that the long-term probability of transmission should fall to close to zero. This is similar to the predictions of the Ricker model, which always returns to zero after the peak (Bolker 2008). Peak transmission occurred at similar times for the Resistant (8.6 weeks) and Susceptible (9.0 weeks) genotypes (Fig. 5d). Comparing transmission between years, the peak transmission in 2017 was later and lower than in 2016 for both genotypes (Figs. 5c and 5d).

We used elastic net to assess the best set of explanatory variables that explained infection status of test plants (i.e., transmission). The set of regularization parameter estimates selected most frequently (mode) from cross-validation were $\alpha = 0$ and $\lambda = 5.46$ in 2016, and $\alpha = 0.1$, $\lambda = 0.99$ in 2017. When $\alpha = 0$, elastic net simplifies to ridge regression. That our estimates of α are close to or equal to 0 suggests strong co-variance among explanatory variables (James et al. 2013). The set of explanatory variables with consistently non-zero coefficient estimates were: presence of *PdR1* resistance trait (i.e., whether the source plant was Resistant or Susceptible), proportion of vectors infectious with *X. fastidiosa* (i.e., acquisition rate), and leaving rates from test plants (Fig. 6). In 2016, the presence of *PdR1* resistance trait was the best predictor, with leaving rates from the test plant being the second strongest predictor. In 2017, proportion of vectors infectious with *X. fastidiosa* was the best predictor; again, leaving rates from test plants was the second strongest predictor. In 2016, the coefficient estimate of the Resistant trait covariate was positive, whereas it was negative in 2017, indicating greater overall transmission from Susceptible plants in 2016 and greater overall transmission from Resistant plants in 2017.

Analysis of secondary metabolites

We isolated 105 distinct secondary metabolites from our source plants: 20 phenolics from leaf blades, 21 phenolics from stems, and 64 volatiles from leaf blades, 28 of which were unidentified. Because of this large number of compounds, we tested for broad differences in total concentrations among these two classes (phenolics and volatiles) and two tissues (leaf blades and stems) using MANOVA. We could not detect any clear change in concentrations of phenolic and volatile secondary metabolites over time (Pillai's trace = 0.157, $F_{3,45} = 2.80$, $P = 0.051$). However, we found that phenolics and volatiles clearly differed between Resistant and Susceptible source plants (Pillai's trace = 0.241, $F_{3,45} = 4.76$, $P = 0.0058$) and this difference increased over time (Fig. 6; interaction of resistance status by weeks post-inoculation: Pillai's trace = 0.229, $F_{3,45} = 4.46$, $P = 0.0079$). This was more clear for total phenolics and total volatiles in leaf blades than for total phenolics in stems (Fig. 6; *univariate ANOVA tests not shown*).

To explore the phytochemical identities of Resistant and Susceptible source plants in a more unsupervised manner, we extracted principal components for all 105 compounds at each time post-inoculation (Supplementary Material, Appendix C, Fig. C1). Overall, the first two principal components (PCs) captured between 12% and 50% of variation among all compounds, depending on the time point. Susceptible source plants tended to vary more across both PCs with Resistant source plants tending to cluster more tightly and within the variation of the Susceptible plants. However, at eight weeks post-inoculation, Resistant plants showed equivalent amount of variation among replicates. At 14 weeks post-

inoculation, we see clearer separation between Susceptible and Resistant plants in PC1 and PC2 which together explained 64% of total variance (Fig. C1).

We also investigated how different compounds might be associated with our estimates of attraction rates and leaving rates of *G. atropunctata* vectors in each cage using the elastic net algorithm. Here, we included all replicates from both Resistant and Susceptible vines and across all time points; we also included Pierce's disease symptom severity as a predictor. For attraction rates, elastic net selected a subset of 8 secondary metabolites—plus Pierce's disease symptoms—as the best set explaining variation in attraction rates (Fig. C2). Pierce's disease symptom severity was the single best predictor of attraction rates, and negatively so. Some secondary metabolites that were negatively associated with attraction rates included vitisin A, kaempferol hexoside galactoside, isogeraniol, and quercetin-3-O-glucoside in leaves. On the other hand, the only compound that was clearly positively associated with attraction rates was coumaric acid 1. For leaving rates, the best value for the elastic net mixing parameter was $\alpha = 0$, simplifying the algorithm to a ridge regression model and leading to no predictors being dropped from the final model. This suggests that the algorithm could not eliminate any compounds as having an effect on leaving rates. Nonetheless, examining the magnitude of coefficient estimates can provide some insight. Leaving rates were positively associated with quercetin-O-3-glucoside in stems, miyabenol C, unidentified volatile S, and unidentified volatile 6; leaving rates were negatively associated with vanillic acid glycoside, caffeic acid glycoside, and unidentified volatile 9 (Appendix C, Fig. C3).

Reinfection experiment

In 2017, we tested for differences in population size of *X. fastidiosa* after either one or two inoculation events, spaced 17 weeks apart using all four genotypes. We found a clear overall reduction in population size from 21 weeks from the first inoculation to 26 weeks (coefficient estimate [95% CI] = -0.467 [-0.922, -0.0121]). We were particularly interested in the three-way interaction between week, treatment, and resistance trait. In line with our hypothesis, Resistant genotypes that had been inoculated twice showed the greatest decline in *X. fastidiosa* population size (Fig. 6). However, this trend could not be detected statistically (coefficient estimate [95% CI] = -0.306 [-1.16, 0.547]). Refer to Supplemental Material Figure S1 for the full timeseries of *X. fastidiosa* population data.

Bio-economic model of PdR1 vineyard

In our simulations, we predict that growers who adopt a more short-term strategy—meaning that they are primarily focused on maximizing returns in a shorter time frame—should not plant *PdR1* vines but should only plant susceptible vines (Fig. 8). However, growers who adopt a more long-term strategy should plant a mixture of *PdR1* and susceptible vines. Generally, the longer the harvest time, the greater the area that growers should plant to *PdR1* vines. These results should clearly depend on the epidemiological conditions experienced by growers. For future research, we are interested in investigating how different epidemiological conditions, motivated by our experimental results, will change optimal planting mixtures as well.

Discussion

Vector-borne plant pathogens present serious threats to agricultural, horticultural, and silvicultural sustainability, as well as plant conservation (Gilligan 2008). Vector suppression through insecticide use is a common management strategy. However, given the harms from insecticides to insect biodiversity and ecosystem services as well as the questionable efficacy of insecticide use (Perring et al. 1999), development of resistant cultivars for agricultural and horticultural provides an important management alternative. At the same time, previous theoretical work has highlighted that the precise form of defense is key: partially resistant or tolerant cultivars could increase the risk of disease spread and spillover (Zeilinger and Daugherty 2014; Sisterson and Stenger 2018).

We applied this theory to characterize defensive traits conferred by the *PdR1* gene in grapevines against *X. fastidiosa* and provide insights into the epidemiological effects of managing Pierce's disease with *PdR1* grapevines. To do so, we compared *X. fastidiosa* populations, Pierce's disease symptoms,

vector preference, vector acquisition, and transmission between *PdRI* resistant and susceptible genotypes over time. We confirmed previous findings that *PdRI* grapevines exhibit reduce symptom severity and harbor lower *X. fastidiosa* populations than susceptible genotypes (Krivanek and Walker 2005; Krivanek et al. 2005; Fritschi et al. 2007). In addition, we found that *X. fastidiosa* populations declined in *PdRI* vines beginning after eight weeks post-inoculation despite relatively mild symptoms.

To study host selection by *G. atropunctata* vectors, we examined both attraction and leaving rates between infected source plants and *X. fastidiosa* test plants. In 2016, we found few indications of preference between infected and healthy plants. However, in 2017, we found consistent evidence that *G. atropunctata* avoided infected Susceptible plants but only when disease symptoms became severe. All previous studies of preference of *X. fastidiosa* vectors found avoidance of symptomatic hosts (Marucci et al. 2005; Daugherty et al. 2017), including *G. atropunctata* (Daugherty et al. 2011). Early in the experiments, we found no preference, corroborating previous work showing that cicadellid vectors of *X. fastidiosa* do not distinguish between non-infected and asymptomatic infected hosts (Marucci et al. 2005; De Miranda et al. 2013). We also found that preference was more strongly realized through greater attraction rates to non-infected hosts, corroborating previous findings that cicadellid vectors orient using visual cues (Rashed et al. 2011; Daugherty et al. 2011). With infected *PdRI* Resistant plants, we saw no differences in preference except at eight weeks post-inoculation in 2017. Here found greater attraction to healthy plants, suggesting a mechanism other than visual cues since disease symptoms were minimal.

Vector acquisition rates—measured as the proportion of vectors that became infectious—were clearly non-linear over the course of disease progression, following unimodal dynamics. The best unimodal model depended more on year than Resistant/Susceptible genotype: the Ricker model was best in 2016 and the Holling Type IV was best in 2017. The Ricker model returns to zero after the peak (Bolker 2008), suggesting that, in 2016, acquisition rates should reach zero over the long term. In contrast, in the Holling Type IV model, the long term dynamics are determined by the parameter a ; the estimate of a for Susceptible genotype trials was more than double the estimate for the Resistant genotype trials suggesting that long-term acquisition would be much greater from Susceptible plants. While vector acquisition rates were consistently greater from Susceptible plants, the difference was clear only in 2017.

As with acquisition rates, vector transmission rates—measured as the proportion of healthy test plants that became infected—were also non-linear, following unimodal dynamics. In 2016, the Ricker model was the best model for both genotypes, peak transmission rate was similar between genotypes, but transmission from Resistant plants peaked earlier and declined faster. In 2017, the Ricker model was again the best model for transmission from Susceptible plants but the Holling Type IV was best for Resistant plant trials, suggesting qualitatively different dynamics. Transmission from Resistant plants may continue over the long term, though at very low rates. The timing of peak transmission was similar between genotypes but the peak transmission rate was nearly double from Resistant plants as from Susceptible plants. Note, however, that the separation in fits among models, based on AIC_c scores, was not as clear for transmission as for acquisition (Tables B2 and B4). Interestingly, the peak transmission rate from Resistant plants coincided with evidence that *G. atropunctata* vectors avoided Resistant infected plants. Both acquisition and transmission rates were consistently lower in 2017 than 2016, likely because we ran trials for eight days in 2016 but for only four days in 2017, reducing the time for both acquisition and transmission.

Contrary to predictions from theory (Fig. 1; Daugherty et al. 2017), we saw unimodal dynamics in transmission from both Susceptible and *PdRI* Resistant grapevines. However, the available evidence suggests distinct mechanisms underlying these similar patterns. For transmission from Susceptible vines, our results broadly conform to our predictions of unimodal transmission dynamics: transmission increases early after inoculation coinciding with increasing population size of *X. fastidiosa*, then declines with increasing symptom severity and concomitant avoidance by vectors. For trials with Resistant vines, because of a lack of symptom development, the unimodal dynamics appear to be more strongly tied to *X. fastidiosa* population size; specifically, transmission appears to decline in later stages of infection because of declining *X. fastidiosa* population size. We saw substantial declines in population size after eight weeks post-inoculation in two of the three resistant genotypes that we tested—genotype 006 in 2016 and

genotype 102 in 2017. Based on the available evidence, we suggest that *PdR1* gene may confer both partial resistance and partial tolerance against *X. fastidiosa*.

The unexpected findings of apparently induced resistance after eight weeks post-inoculation led us to test this further with a re-infection experiment, where we compared *X. fastidiosa* population size in Resistant and Susceptible vines after inoculating plants either only once or again at 17 weeks post-inoculation. We hypothesized that Resistant vines that had previously been inoculated would show the greatest reduction in *X. fastidiosa* population size. While the trends in our data support this hypothesis, we were unable to clearly distinguish Resistant vines that had been inoculated twice vs. only once. This could be due to our small sample size, but also could be explained if the apparently late-season resistance was induced by phenology rather than prior exposure to *X. fastidiosa*.

While our re-infection study results were suggestive but inconclusive, our multivariate analysis of secondary metabolites showed that at 14 weeks post-inoculation Resistant grapevines clearly differed from Susceptible grapevines. Resistant vines had about half the total concentration of phenolic and volatile compounds in leaves relative to Susceptible vines. Additionally our PCA analysis showed much greater separation of Resistant and Susceptible vines at 14 weeks than at any other time point. Wallis et al. (2013) showed that concentrations of phenolic compounds in grapevine xylem tissue increased steadily throughout the season regardless of cultivar or *X. fastidiosa* infection status. In contrast, phenolic compounds in our infected *PdR1* Resistant plants were greatest early in our experiment and plateaued later. Importantly, disease symptom severity (or lack thereof) was the single strongest predictor of vector attraction rates in our elastic net analysis, further corroborating our analysis and previous studies that *G. atropunctata* primarily uses visual cues to orient toward host plants (Daugherty et al. 2011).

Recent theoretical work on the epidemiology of vector-borne plant diseases has emphasized the importance of vector behavior—specifically host selection behavior based on host infection status (McElhany et al. 1995; Sisterson 2008; Roosien et al. 2013; Shaw et al. 2017; Gandon 2018; Donnelly et al. 2019; Shoemaker et al. 2019). Meanwhile experimental work has succeeded in documenting a wide variety of infection-induced host selection behaviors in vectors (reviewed in Eigenbrode et al. 2018). However, to our knowledge, no study has yet to quantitatively test for an empirical relationship between infection-induced host selection and vector transmission. A few studies have suggested a positive association (Daugherty et al. 2011, 2017; Del Cid et al. 2018), but the findings of Jennersten (1988) suggest that vector preference does not predict transmission. Furthermore, disentangling which components of host selection behavior by vectors is most important for transmission would help to focus both theoretical and experimental work.

We tested the relationship between transmission and the different components of vector feeding preference using estimates of attraction and leaving rates to/from both infected and non-infected hosts. These estimates were calculated from fitting the consumer movement model of Zeilinger et al. (2014) to our repeated measures dataset of vector location. The model provides estimates of these components of preference from a single experiment, enabling transmission to be measured concurrently. We once again used elastic net to assess the relative influence of each component of preference as well as other epidemiological parameters on transmission. Elastic net is ideal for statistical problems where one's goal is variable selection among a set of co-varying predictors, as will likely be the case with any vector transmission experiment (James et al. 2013). It also provides conservative coefficient estimates compared to ordinary least squares regression, biasing estimates towards zero in order to reduce variance (James et al. 2013). From this analysis, we found that resistance trait (use of Resistant or Susceptible genotype), vector acquisition rate, and leaving rate from the non-infected plant were the most important predictors of transmission rate. These patterns were consistent over the both years of our experiment. The importance of leaving rate from healthy hosts supports the conclusions of (Nault and Ammar 1989), who suggested that transmission of persistent viruses was sensitive to tenure time on healthy hosts (where tenure time = leaving rate⁻¹). Our findings appear to contradict the theoretical results of Shaw et al. (2017), who predicted that acquisition rate (β , in their model) and leaving rate of infectious vectors from non-infected hosts (a_h and c_2) had negligible influence on disease spread of persistently transmitted pathogens. At the same time, it's possible that the influence of leaving rates and acquisition rates are bound up in other

parameters in the model of Shaw et al. (2017). For example, the importance of leaving rate from non-infected plants in our experiment is likely because of its relationship with inoculation rate, which Shaw et al. (2017) predicted would be highly influential on spread. In addition, our analysis suggests that attraction rate to source plant has relatively little impact on transmission, contrary to the models of Sisterson (2008) and Shaw et al. (2017). However, the reduced attraction rates to infected plants we observed seem to be the only plausible explanation for our observed declines in transmission from Susceptible plants. And attraction rate to infected plants may be so closely tied with acquisition rate that our analysis was unable to partition variance to these different predictors effectively.

Vector attraction rates and leaving rates were clearly important in driving transmission dynamics of *X. fastidiosa* in our system. We observed reduced attraction rates toward diseased Susceptible plants that clearly coincided with a decline in transmission consistent with theory (Daugherty et al. 2017). At the same time, our results overall suggest that vector preference alone does not predict transmission, and can be misleading at times. For example, we detected reduced attraction rates toward Resistant source plants at eight weeks post-inoculation in our 2017 experiment. While we would again expect reduced transmission rates, we instead observed the highest transmission rates during that year's experiment.

The apparent inconsistencies of our results with theory are intriguing but may also relate to peculiarities of *X. fastidiosa* pathosystems. Most theory on vector feeding preference appears to be motivated by aphid-borne phloem-colonizing virus systems. As a xylem-limited bacterial pathogen, host plant responses to infection are likely to be quite different from phloem-colonizing viruses and other pathogens. Plant responses are likely to mediate much of the transmission dynamics shown here and in other studies (Blua and Perring 1992; Werner et al. 2009). More quantitative tests of the relationships between the components of vector feeding preference and transmission in a variety of systems will be critical to assessing the generality and explanatory power of current theory.

While the use of resistant cultivars is a key component to integrated disease management in agriculture, such cultivars need to be assessed to ensure that they do not increase the risk of spillover or epidemics. Based on the available theory and our results, the greatest risk of transmission of vector-borne plant pathogens should occur within a window of disease progression when both pathogen burden and attractiveness to the vector are high (De Moraes et al. 2014). These two processes are clearly dynamic and may be governed by different mechanisms. For disease systems where vectors avoid symptomatic hosts, such as *X. fastidiosa*-associated diseases, the duration of the incubation period—in which hosts are infectious but asymptomatic—should be the period of greatest vector acquisition (Daugherty et al. 2017). Tolerance traits or even partial resistance traits could potentially extend the duration of the incubation period, increasing the risk of pathogen spread. Numerous other factors are likely to influence the duration of the incubation period, including water stress and temperature (Daugherty et al. 2017; Del Cid et al. 2018).

Our results indicate that *PdRI* hybrid grapevines can produce transmission rates greater than those from susceptible vines, potentially posing a risk of enhancing spread of *X. fastidiosa*. However, our results also suggest that these higher transmission rates may be transient, followed by transmission rates similar or lower than those from susceptible plants. This may be due to some form of induced resistance in the plants, though our attempts to quantify the form of resistance were inconclusive. Riaz et al. (2018) hypothesize that *PdRI* could confer a form of “non-host resistance,” a set of constitutive and induced traits that provide broad general resistance against pathogens (Senthil-Kumar and Mysore 2013). Such general resistance mechanisms include induction of phenolics through the hypersensitive response and the salicylic acid signaling pathway. Phenolic induction is associated with *X. fastidiosa* populations in olive trees and grapevines, although phenolic levels tend to be greater in susceptible cultivars rather than resistant ones (Wallis and Chen 2012; Luvisi et al. 2017). Additionally, Fritschi et al. (2007) found unimodal *X. fastidiosa* population dynamics in a range of *Vitis* spp. with varying levels of resistance, including an accession of *V. arizonica* related to the parental background of our *PdRI* vines; they suggested that such unimodal dynamics could be caused by induced resistance.

In the current study we sought to assess the existence or possibility of an epidemic risk from *PdRI* grapevines. Further work will need to be done to examine the factors that could contribute to

shortening or broadening the incubation period, and thus the epidemic risk. Additional work should also look at the potential use of *PdRI* vines in regions with high winter recovery of grapevines—where *X. fastidiosa* populations are eliminated in the vine over the winter. Winter recovery appears to be most likely in cases when *X. fastidiosa* has not yet systemically colonized the plant and under cold winter temperatures (Feil et al. 2003). We would expect the dynamics in our study to play out at a longer timescale for much larger mature vines in the field. *PdRI* induced resistance could increase rates of winter recovery and substantially lower annual build-up of disease pressure. Moreover, the seasonal timing of the incubation period and peak vector acquisition is critically important for determining the epidemic risk (Daugherty and Almeida 2019).

Our bioeconomic model results assumed no winter recovery. We hypothesize that incorporating winter recovery into the model will lead to a broader set of epidemiological and economic conditions under which planting a mixture of *PdRI* and susceptible grapevines would maximize grower return; for example, winter recovery may lead to planting *PdRI* being beneficial under short-term planting strategies.

Acknowledgements

We thank Alan Tenschler for help with selecting and propagating grapevines; we thank Michael Voeltz, Jeffery Ezennia, Bitta Kahangi, Melissa Shinfuku, Jon Oules, Sanjeet Paluru, Tina Wistrom, and Sandy Purcell for help with maintaining grapevines and insect colonies, and conducting experimental work. Summaira Riaz, Matthew Daugherty, and members of the Almeida lab provided useful comments on results and early manuscript drafts.

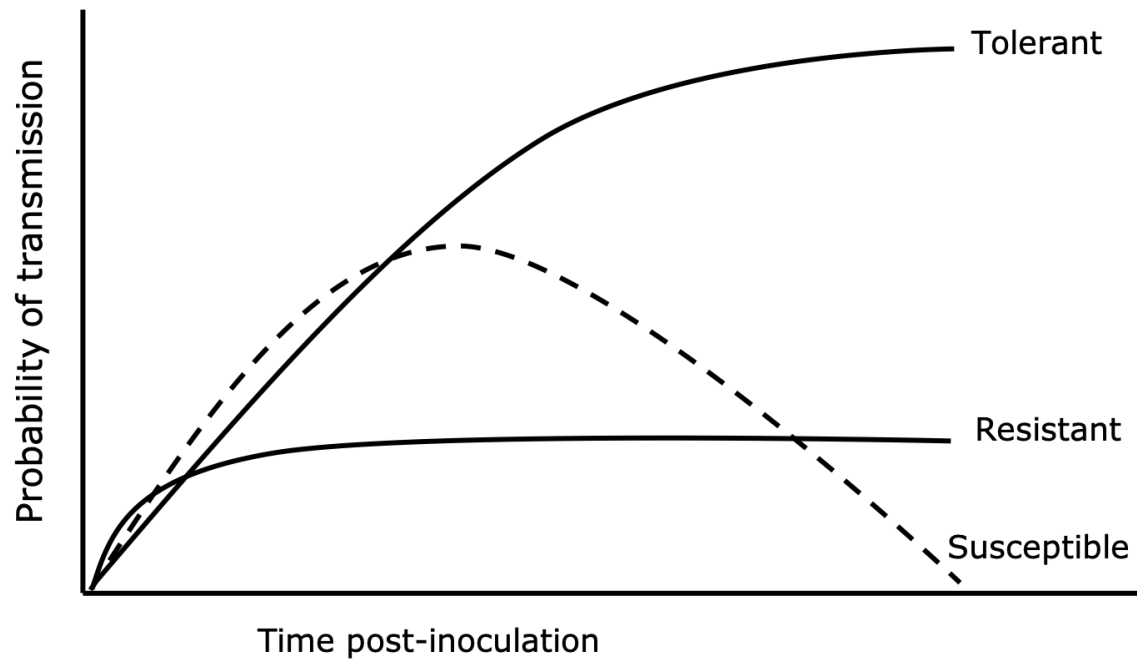


Figure 1. Theoretical predictions on vector transmission dynamics in the context of plant host defense (or lack thereof) and vector avoidance of symptomatic hosts. Here we assume resistance is partial, meaning that the pathogen can colonize the host but population growth is limited. The decline in transmission from Susceptible hosts is predicted to correspond to increasing vector avoidance of symptomatic plants.

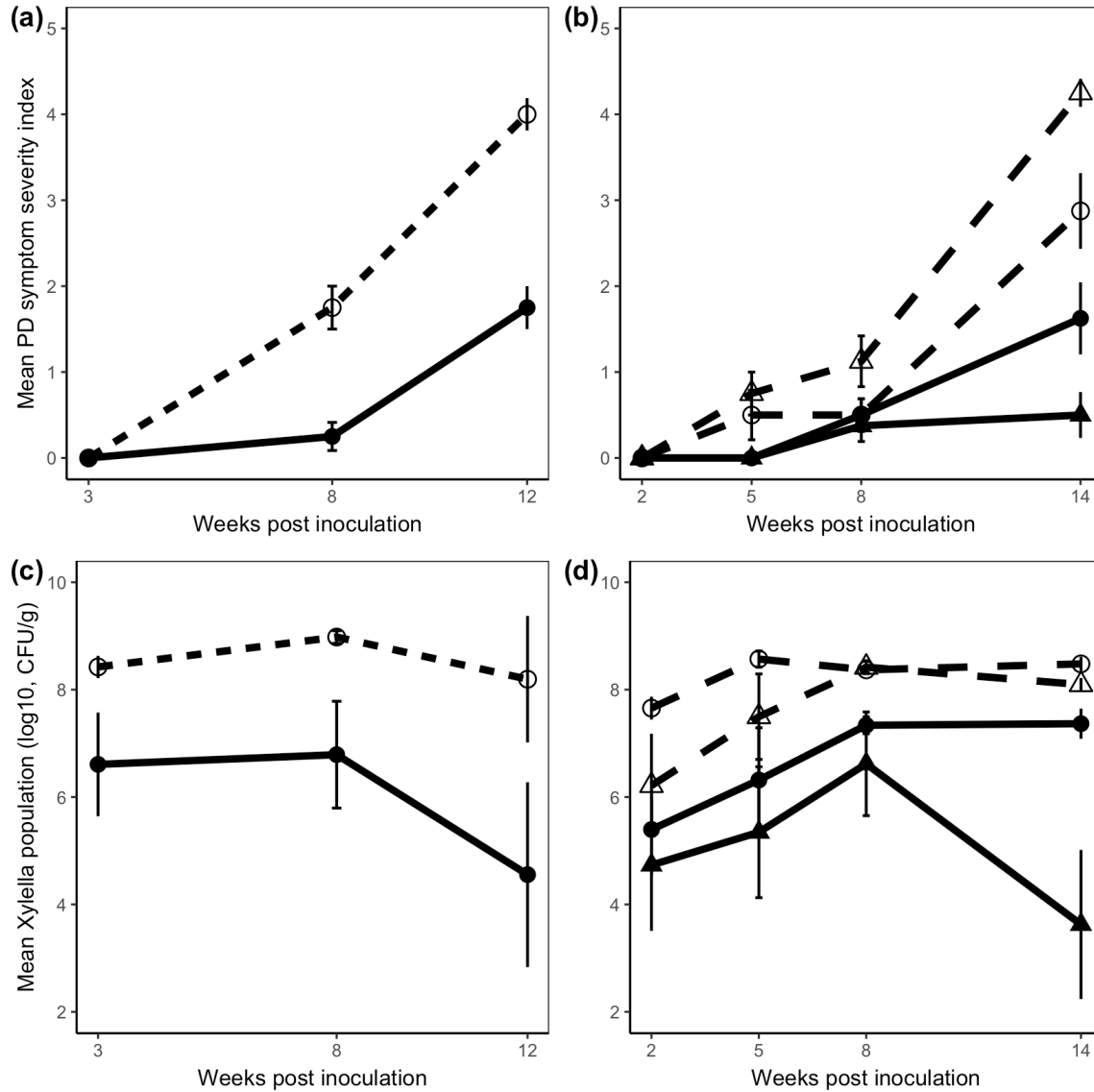


Figure 2. Mean \pm SE Pierce's disease symptom severity index (a, b) and mean \pm SE population sizes of *X. fastidiosa* in inoculated source plants (c,d) for Susceptible genotypes (open symbols, dashed lines) and Resistant genotypes (closed symbols, solid lines) over time. Population sizes are log₁₀ transformed and expressed as colony forming units (CFU) g⁻¹ fresh plant tissue.

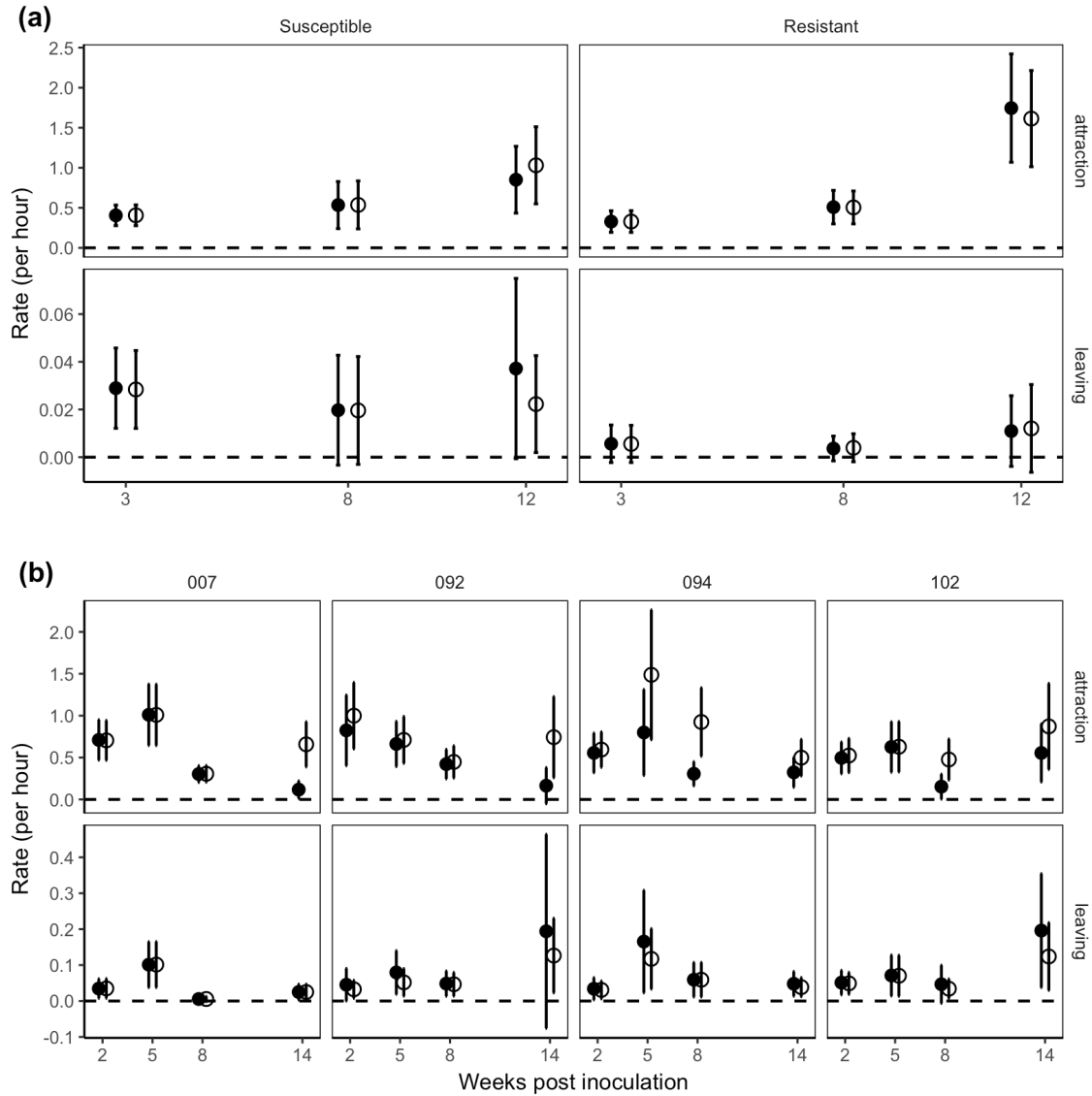


Figure 3. Results of *G. atropunctata* vector feeding preference for inoculated source grapevines (closed circles) and *X. fastidiosa*-free test plants (open circles) over weeks post-inoculation for experiments in (a) 2016 and (b) 2017. Top sub-panels show attraction rate estimates; bottom sub-panels show leaving rate estimates. Genotypes are shown at the top of each set of sub-panels. In 2017, genotypes 007 and 092 are Susceptible lines; genotypes 094 and 102 are Resistant lines. Maximum likelihood estimates (points) and variances were model-averaged using AIC_c weights. Variances were calculated using the quadratic approximation method and then used to calculate 95% confidence intervals (error bars).

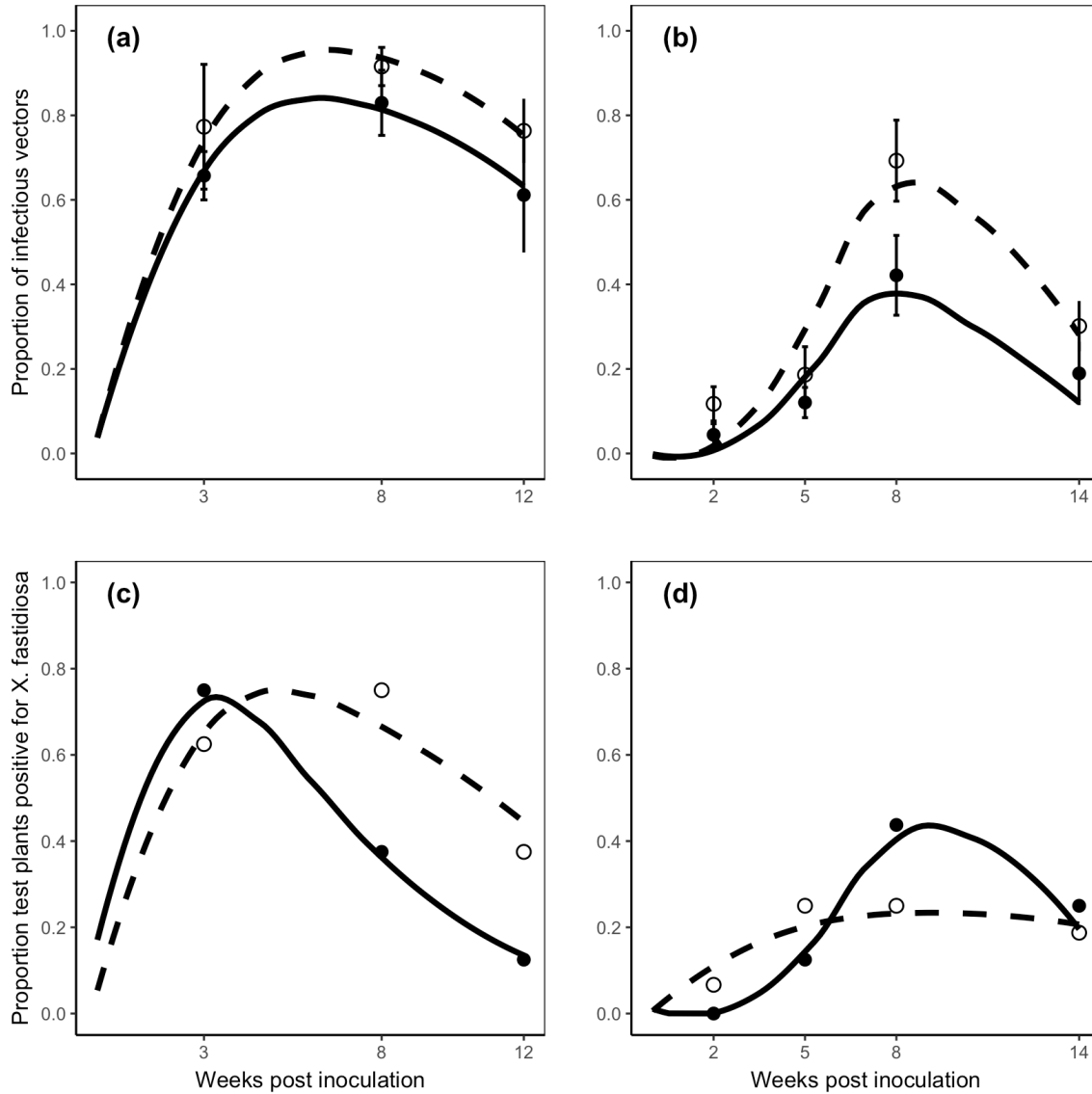


Figure 4. Vector acquisition of *X. fastidiosa* (a, b) and transmission to test plants (c, d) from Susceptible (open circles, dashed lines) and Resistant (closed circles, solid lines) inoculated source plants in 2016 (a, c) and 2017 (b, d) experiments. Lines represent predictions from best non-linear model based on AIC_c scores. In (a) and (b), points and error bars represent mean and SE, respectively, of the proportion of vectors positive for *X. fastidiosa*.

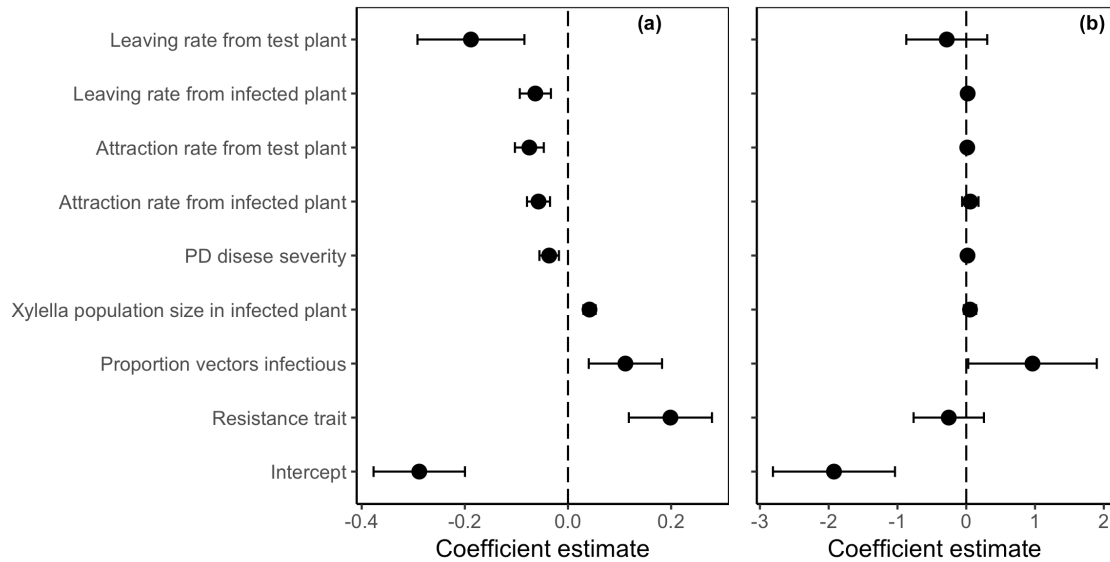


Figure 5. Mean coefficient estimates \pm SD from elastic net analysis of the relationship between explanatory variables, on the y-axis, and infection status of test plant (i.e., probability of transmission). The “Resistance trait” variable indicates a binomial variable where trials with Resistant source plants are coded as “0” and trials with Susceptible source plants are coded as “1”; thus a positive coefficient indicates greater overall transmission from Susceptible plants. Attraction and leaving rates are estimated for each trial using the Consumer Movement Model described in the full text. Means and standard deviations were calculated from 500 cross-validation runs.

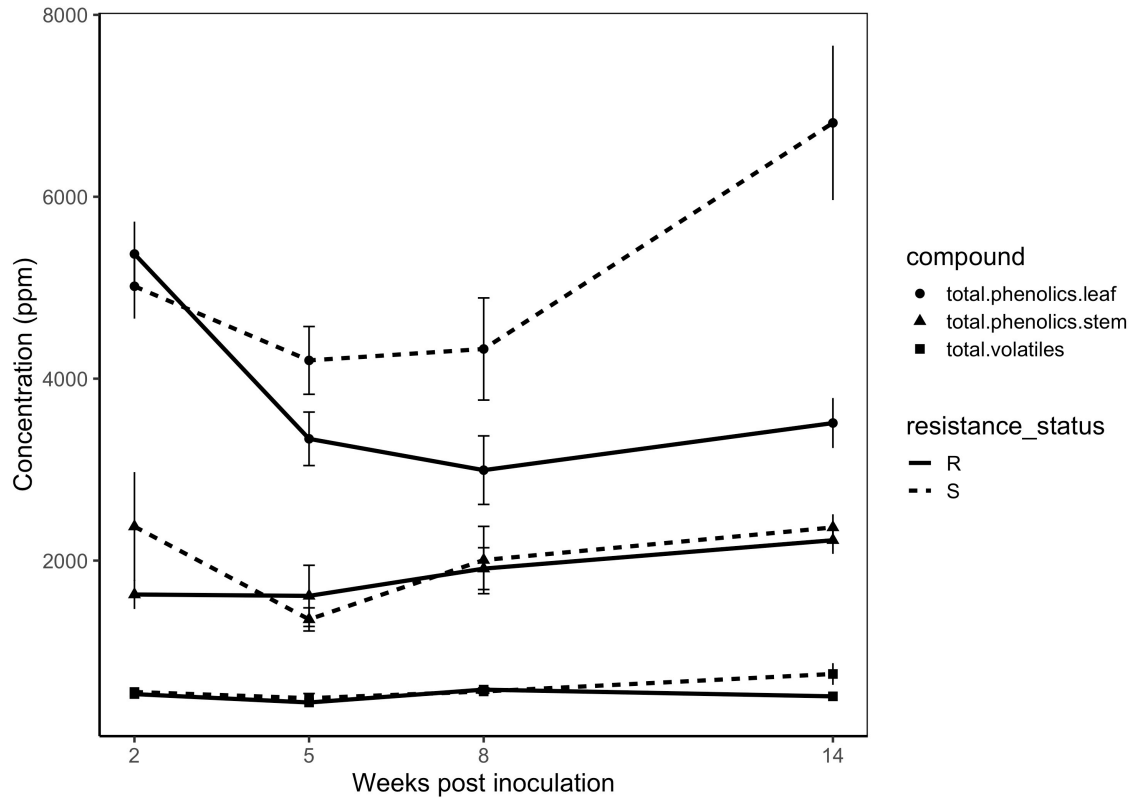


Figure 6. Mean concentrations (ppm) of all phenolics in leaves and stems and volatiles in leaves from Resistant (R) and Susceptible (S) source plants at different times since inoculation with *X. fastidiosa*. Sample size for each point estimate varies from 4 – 8; see PCA ordination plots (Supplementary Material, Appendix C, Fig. C1) for specific sample sizes of each point. Error bars represent \pm SE.

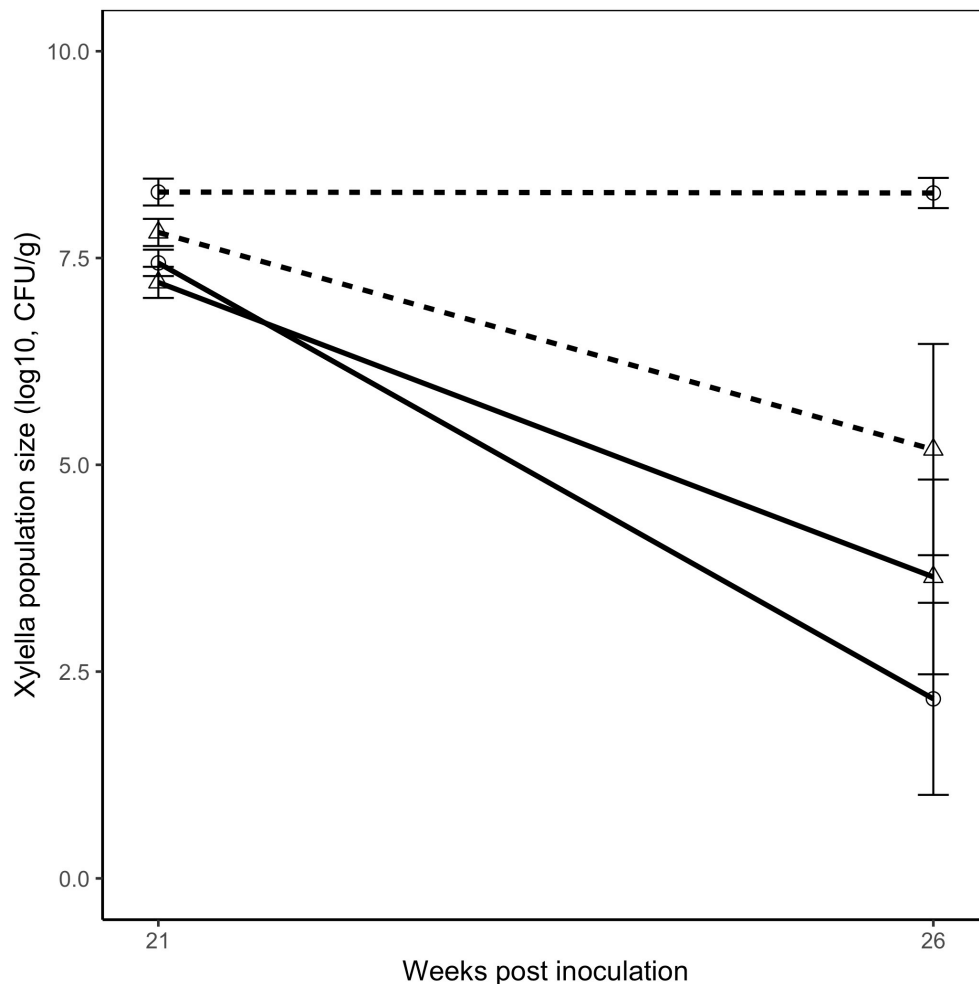
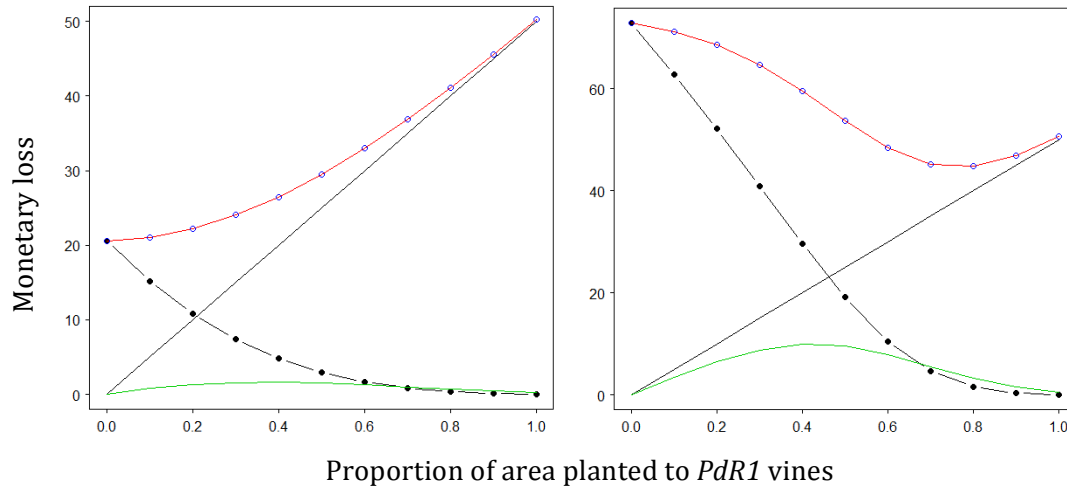


Figure 7. Mean population size of *X. fastidiosa* in needle-inoculated Resistant (solid line) and Susceptible (dashed lines) grapevines. Plants were either inoculated twice (open circles) or inoculated once (open triangles). The weeks post-inoculation on the x-axis represent the weeks since the first inoculations. The second inoculation was conducted 17 weeks after the first. Thus population sizes were measured 4 and 9 weeks after the second inoculation. N = 4 for each treatment and resistance combination. Error bars represent ± SE.

Figure 8. Optimal mixture of susceptible and *PdR1* vines corresponds to the minimum total monetary loss, represented by the red line. Black solid line: loss due to planting. Dashed line: loss due to infection for susceptible vines. Green line: loss due to infection for *PdR1* vines. Red line: total loss (blue points are calculated by subtracting a profit calculated from the final number of healthy plants from the maximum possible profit). Left panel: harvest at $t = 50$ time steps, right panel: harvest at $t = 80$ time steps.



Supplementary Information Appendix A. Testing assumptions and model selection results for consumer movement model.

Testing model assumptions

To interrogate the assumptions of the consumer movement model, we set up a similar to the 2017 preference-transmission experiment as described in the main text, except that the source plants were all susceptible genotype 007 at 15 weeks post-inoculation and only a single BGSS individual was placed in each cage. We began with 16 replicates with six insects dying in the course of the experiments.

First, the model assumes that attraction and leaving rates were constant throughout the experiment. We interrogated this assumption by graphical inspection of the outputs of Kaplan-Meier survival functions as described in Zeilinger et al. (2014). While there are few points—indicating relatively little movement between plants by BGSS—the plots suggest that attraction rates and leaving rates were roughly constant, with the exception of leaving rates from *X. fastidiosa*-inoculated source plants (Fig. A1).

Second, the model assumes that consecutive choices made by BGSS are independent. While this assumption can be interrogated by contingency table analysis, there were too few data points to support such an analysis. Rather, we opted to inspect the variance-covariance matrices from the best model variant from the output of maximum likelihood estimation for the main transmission experiment.

For the 2016 trials, correlations between parameters varied substantially; about 60% of correlations were below 0.5, suggesting modest independence among choices (Table A1). For 2017, about 40% of correlations between parameters were below 0.5, suggesting less independence among choices (Table A2).

While the assumption of independent consecutive choices was not met in all cases, this does not necessarily invalidate results from the Consumer Movement Model. Rather, non-independence among choices is likely to inflate attraction rates (Zeilinger et al. 2015). In nearly all instances, correlations—and thus the degree of inflation of attraction rates—were symmetrical between choices. The exceptions to this were in 2017 for 8- and 14-week trials with the 094 Resistant genotype (“8-094” and “14-094” entries; Table A2). In these instances, the leaving rate from both plants, μ , had a much higher correlation with the attraction rate toward the uninfected test plant, p_2 , than with the attraction rate toward the source plant, p_1 . In both cases, our estimates of the attraction rates suggest greater attraction toward the test plant than the source plant, significantly so in the 8-week trials (Fig. 3, main text). It remains unclear to what degree this large difference in attraction may be an artifact of non-independent choices.

The generalization of the model for multiple consumers per cage also assumes that each consumer makes choices independent of others in the cage (Gray et al. *in review*). While no published research exists on independence of host plant choices of *G. atropunctata*, unpublished data suggest that choices are independent of conspecifics (A. Purcell, *personal communication*).

Model selection results

We fit four variants of the Consumer Movement Model to repeated-measures *G. atropunctata* count data from each genotype and week post-inoculation. Briefly, the four model variants were: 1) the Fixed Model, in which the attraction and leaving rates were set equal to each other, representing a null hypothesis of no preference between choices; 2) the Free Attraction Model, in which the attraction rates to each plant were free to vary but the leaving rates from each were set equal to each other; 3) the Free Leaving Model, in which attraction rates were fixed but leaving rates were free to vary; and 4) the Free Choice Model, in which both the attraction and leaving rates were free to vary. We compared model variants using Akaike’s Information Criterion corrected for small sample size (AIC_c). We then calculated model-averaged parameter estimates and variances using the AIC_c weights of all models with values of $\Delta AIC_c \leq 7$ (Burnham et al. 2011). We then calculated 95% confidence intervals from these model-averaged variances (Fig. 3 main text).

In the 2016 experiment, the Fixed model had the lowest ΔAIC_c for each combination of genotype and weeks, except for the trials with Susceptible source plants at 12 weeks post-inoculation (Table A3).

The Fixed model was clearly the best for most of these trials (i.e., the ΔAIC_c values for the remaining models were > 2), indicating that the *G. atropunctata* showed no preference between infected source plants and *X. fastidiosa*-free test plants. In the trials with Susceptible plants at 12 weeks, the Free Leaving model was the best, closely followed by the Free Attraction model (Table A3). These two models clearly performed better than the Fixed model, indicating that *G. atropunctata* showed a preference between the host plant choices and that this preference was likely realized through different leaving rates.

In the 2017 experiment, patterns of preference were more complicated than in 2016 though the differences were clearer (Table A4). At two weeks post-inoculation, the Fixed model fit the data best overall; while the Fixed model performed slightly worse than the Free Attraction and Free Leaving models for genotype 092 Susceptible trials, the difference was negligible ($\Delta AIC_c < 1$). At five weeks post-inoculation, the Fixed model fit the data best for trials with genotypes 007 Susceptible and 102 Resistant; once again, the Fixed model performed worse than the Free Attraction and Free Leaving models for genotype 092 Susceptible but now the difference in performance was stronger ($\Delta AIC_c > 2$). Interestingly, for genotype 094 Resistant, the Fixed model performed much worse than all other models, with the Free Attraction model performing best. At eight weeks post-inoculation, the Fixed model performed the best for both Susceptible genotypes (007 and 092), whereas the Free Attraction model performed the best for both Resistant genotypes (094 and 102). At 14 weeks post-inoculation, the Free Attraction model performed the best for all genotypes. At the same time, the performance of the Free Attraction model as the best model was much clearer for the Susceptible genotypes than for the Resistant genotypes (Table A4).

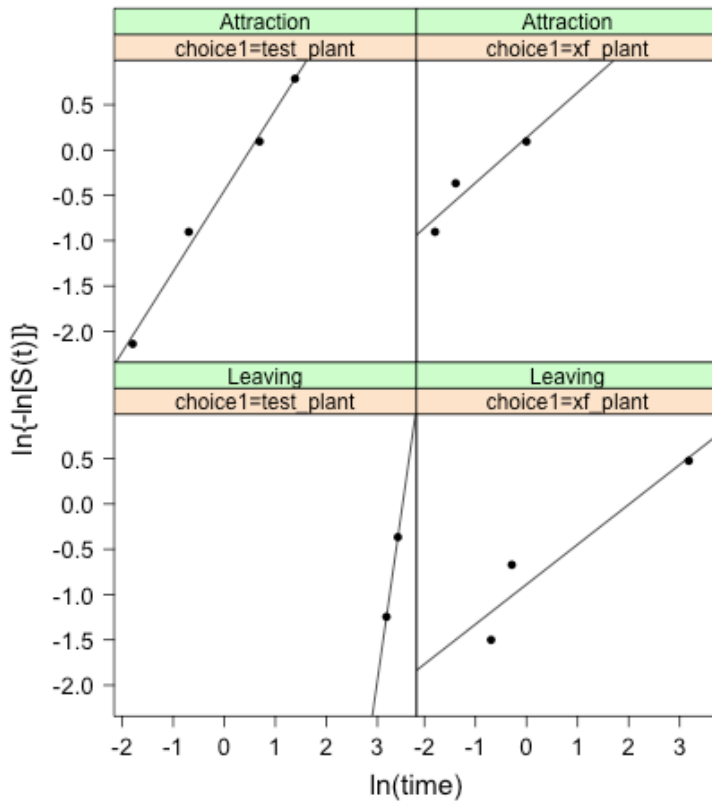


Figure A1. Relationship between $\ln(\text{time})$ and $\ln(-\ln(S(t)))$ from Kaplan-Meier survival functions, where t (or time) represents the time that an attraction or leaving event occurred, and $S(t)$ is the proportion of individuals remaining at time t . A linear relationship suggests that the attraction or leaving rate was constant throughout the experiment. Top panels: attraction rates from *X. fastidiosa*-infected source plants (“xf_plant”) and uninfected test plants (“test_plant”). Bottom panels: leaving rates. Analysis of attraction to and leaving from the insects’ first choice only are shown; too few data existed for subsequent choices for analysis.

Table A1. Correlation matrices among parameters of the Consumer Movement Model for each week-genotype combination from the 2016 transmission experiment.

Week-genotype combination	Correlation matrix			
3-R	p	μ		
	p	1	0.551	
	μ	0.551	1	
3-S	p	μ		
	p	1	0.578	
	μ	0.578	1	
8-R	p	μ		
	p	1	0.269	
	μ	0.269	1	
8-S	p	μ		
	p	1	0.772	
	μ	0.772	1	
12-R	p	μ		
	p	1	0.176	
	μ	0.176	1	
12-S	p	μ_1	μ_2	
	p	1	0.488	0.49
	μ_1	0.488	1	0.882
	μ_2	0.49	0.882	1

R = Resistant; S = Susceptible

Choice 1 (with corresponding p_1 and μ_1 parameters) = *X. fastidiosa*-infected source plants

Choice 2 (with p_2 and μ_2 parameters) = uninfected test plants

Parameters without a numeral (p or μ) represent instances where the parameters associated with both choices were equal.

Table A2. Correlation matrices among parameters of the Consumer Movement Model for each week-genotype combination from the 2017 transmission experiment.

Week-genotype combination	Correlation matrix			
2-007	p	μ		
	p	1	0.506	
	μ	0.506	1	
2-092	p	μ_1	μ_2	
	p	1	0.409	0.399
	μ_1	0.409	1	0.76
	μ_2	0.399	0.76	1
2-094	p	μ		
	p	1	0.508	
	μ	0.508	1	
2-102	p	μ		
	p	1	0.611	
	μ	0.611	1	
5-007	p	μ		
	p	1	0.707	
	μ	0.707	1	
5-092	p	μ_1	μ_2	
	p	1	0.662	0.66
	μ_1	0.662	1	0.867
	μ_2	0.66	0.867	1
5-094	p_1	p_2	μ	
	p_1	1	0.732	0.579
	p_2	0.732	1	0.712
	μ	0.579	0.712	1
5-102	p	μ		
	p	1	0.828	
	μ	0.828	1	
8-007	p	μ		
	p	1	0.254	
	μ	0.254	1	
8-092	p	μ		
	p	1	0.718	
	μ	0.718	1	
8-094	p_1	p_2	μ	
	p_1	1	0.696	0.638
	p_2	0.696	1	0.768

	μ	0.638	0.768	1
8-102	p_1	1	0.457	0.454
	p_2	0.457	1	0.674
	μ	0.454	0.674	1
14-007	p_1	1	0.378	0.564
	p_2	0.378	1	0.578
	μ	0.564	0.578	1
14-092	p_1	1	0.722	0.692
	p_2	0.722	1	0.854
	μ	0.692	0.854	1
14-094	p_1	1	0.491	0.529
	p_2	0.491	1	0.492
	μ	0.529	0.492	1
14-102	p_1	1	0.784	0.714
	p_2	0.784	1	0.802
	μ	0.714	0.802	1

Genotypes 007 and 092 are Susceptible genotypes; 094 and 102 are Resistant genotypes
 NA = Not Available; correlations were inestimable from Hessian matrix.

Choice 1 (with corresponding p_1 and μ_1 parameters) = *X. fastidiosa*-infected source plants

Choice 2 (with p_2 and μ_2 parameters) = uninfected test plants

Parameters without a numeral (p or μ) represent instances where the parameters associated with both choices were equal.

Table A3. Model selection tables for Consumer Movement model variants for each combination of week post-inoculation and genotype for the 2016 transmission experiment.

Week-Genotype combination	Model	AIC _c	ΔAIC _c	df
3-R	Fixed	146.47	0	2
	Free Leaving	152.01	5.54	3
	Free Attraction	152.06	5.59	3
	Free Choice	161.34	14.87	4
3-S	Fixed	171.90	0	2
	Free Leaving	176.47	4.57	3
	Free Attraction	177.46	5.56	3
	Free Choice	183.90	12.00	4
8-R	Fixed	132.33	0	2
	Free Leaving	137.22	4.89	3
	Free Attraction	137.84	5.51	3
	Free Choice	146.54	14.22	4
8-S	Fixed	153.10	0	2
	Free Leaving	158.61	5.51	3
	Free Attraction	158.63	5.53	3
	Free Choice	167.94	14.85	4
12-R	Fixed	145.83	0	2
	Free Attraction	148.75	2.92	3
	Free Leaving	149.49	3.66	3
	Free Choice	157.95	12.12	4
12-S	Free Leaving	158.39	0	3
	Free Attraction	159.81	1.41	3
	Fixed	161.58	3.19	2
	Free Choice	167.52	9.13	4

R = Resistant genotype; S = Susceptible genotype

AIC_c = Aikake's Information Criterion corrected for small sample size

ΔAIC_c = Difference between lowest AIC_c score and a given score

df = degrees of freedom, i.e., number of model parameters

Separate tables are sorted by ΔAIC_c in ascending order

Table A4. Model selection tables for Consumer Movement model variants for each combination of week post-inoculation and genotype for the 2017 transmission experiment.

Week-Genotype combination	Model	AIC _c	ΔAIC _c	df
2-007	Fixed	138.32	0	2
	Free Leaving	143.53	5.21	3
	Free Attraction	143.59	5.27	3
	Free Choice	152.85	14.52	4
2-092	Free Leaving	127.55	0	3
	Free Attraction	127.83	0.28	3
	Fixed	128.43	0.88	2
	Free Choice	136.37	8.82	4
2-094	Fixed	137.87	0	2
	Free Leaving	140.58	2.71	3
	Free Attraction	140.60	2.72	3
	Free Choice	149.65	11.78	4
2-102	Fixed	134.87	0	2
	Free Attraction	137.72	2.84	3
	Free Leaving	138.44	3.57	3
	Free Choice	147.05	12.17	4
5-007	Fixed	141.89	0	2
	Free Leaving	147.42	5.53	3
	Free Attraction	147.47	5.57	3
	Free Choice	156.70	14.80	4
5-092	Free Leaving	151.41	0	3
	Free Attraction	154.30	2.90	3
	Fixed	155.02	3.62	2
	Free Choice	160.37	8.96	4
5-094	Free Attraction	147.77	0	3
	Free Leaving	149.23	1.46	3
	Free Choice	156.34	8.57	4
	Fixed	169.29	21.51	2
5-102	Fixed	161.38	0	2
	Free Leaving	166.20	4.82	3
	Free Attraction	166.67	5.30	3
	Free Choice	174.68	13.3	4
8-007	Fixed	129.41	0	2
	Free Attraction	134.83	5.41	3
	Free Leaving	135.01	5.60	3
	Free Choice	144.11	14.7	4
8-092	Fixed	148.86	0	2
	Free Attraction	151.50	2.64	3

	Free Leaving	152.37	3.50	3
	Free Choice	160.73	11.87	4
8-094	Free Attraction	170.06	0	3
	Free Choice	178.47	8.41	4
	Free Leaving	181.82	11.76	3
	Fixed	184.15	14.09	2
8-102	Free Attraction	135.96	0	3
	Free Leaving	139.16	3.20	3
	Free Choice	144.13	8.17	4
	Fixed	154.92	18.96	2
14-007	Free Attraction	128.15	0	3
	Free Choice	137.46	9.31	4
	Free Leaving	138.13	9.98	3
	Fixed	144.90	16.74	2
14-092	Free Attraction	149.60	0	3
	Free Leaving	152.69	3.09	3
	Free Choice	156.75	7.15	4
	Fixed	190.25	40.65	2
14-094	Free Attraction	136.05	0	3
	Free Leaving	137.68	1.63	3
	Fixed	140.87	4.82	2
	Free Choice	145.33	9.27	4
14-102	Free Attraction	149.07	0	3
	Free Leaving	149.25	0.18	3
	Free Choice	157.51	8.44	4
	Fixed	168.32	19.25	2

Genotypes 007 and 092 are Susceptible genotypes; 094 and 102 are Resistant genotypes
 AIC_c = Aikake's Information Criterion corrected for small sample size
 ΔAIC_c = Difference between lowest AIC_c score and a given score
df = degrees of freedom, i.e., number of model parameters
Separate tables are sorted by ΔAIC_c in ascending order

Supplementary Information Appendix B. Description and Results of Fitting Non-linear Models

Methods for fitting non-linear models

As described in the main text, we fit a series of non-linear models to our data on vector acquisition and transmission in our 2016 and 2017 experiments. The models are described in Table B1. For a review describing each model, see Bolker (2008).

For vector acquisition data, the response variable was the number of vectors infected with *X. fastidiosa* out of the total vectors recovered from each cage; for transmission data, the response variable was the infection status of each test plant. In both cases, we assumed that the response variable was binomially distributed and the explanatory variable was weeks post-inoculation. We estimated the parameters of each model from the data using maximum likelihood estimation and the R package *bbmle* (Bolker and R Core Team 2017). We selected the best model based on Aikake's Information Criterion corrected for small sample size (AIC_c). Statistical inference was made from 95% confidence intervals of parameter estimates calculated using the quadratic approximation method (Bolker 2008). In 2017, to maximize sample size and statistical power, we tested the Resistant and Susceptible genotypes separately; in other words, we selected the best model for both Resistant genotypes together and did the same for both Susceptible genotypes together.

Table B1. Description of non-linear models used in fitting vector acquisition and transmission data.

Model name	Equation	Functional form	Mathematical family
Holling Type IV	$y = \frac{ax^2}{b + cx + x^2}$	Unimodal	Rational
Ricker	$y = axe^{-bx}$	Unimodal	Exponential
Michaelis-Menten	$y = \frac{ax}{b + x}$	Saturating	Rational
Logistic Growth	$y = \frac{1}{1 + e^{-(a+bx)}}$	Saturating	Exponential
Linear	$y = a + bx$	Linear	Polynomial

In model equations, the variable y represents either the proportion of vectors infected with *X. fastidiosa* or the infection status of the test plant in each trial, whereas x represents weeks post-inoculation. While we use the same symbol/letter to represent the parameters in each equation, parameters among models with the same symbol are not directly comparable. We followed the parameterizations of the models described in (Bolker 2008).

Table B2. Results on model selection among non-linear models of vector acquisition.

Genotype-Year	Model	AIC _c	ΔAIC _c	df
Resistant-2016	Ricker	15.49	0	2
	Holling Type IV	17.71	2.21	3
	Logistic Growth	18.87	3.38	2
	Linear	19.09	3.59	2
	Michaelis-Menten	20.07	4.58	2
Susceptible-2016	Ricker	15.41	0	2
	Holling Type IV	17.63	2.21	3
	Michaelis-Menten	22.95	7.54	2
	Logistic Growth	23.70	8.29	2
	Linear	23.71	8.29	2
Resistant-2017	Holling Type IV	32.13	0	3
	Ricker	56.70	24.58	2
	Michaelis-Menten	62.26	30.13	2
	Linear	71.56	39.44	2
	Logistic Growth	74.55	42.43	2
Susceptible-2017	Holling Type IV	59.73	0	3
	Ricker	85.56	25.83	2
	Michaelis-Menten	94.61	34.88	2
	Linear	109.31	49.58	2
	Logistic Growth	112.50	52.77	2

AIC_c = Aikake's Information Criterion corrected for small sample size

ΔAIC_c = Difference between lowest AIC_c score and a given score

df = degrees of freedom, also the number of parameters

Table B3. Parameter estimates and 95% confidence intervals from best models for vector acquisition.

Genotype-Year	Model	Parameter	Estimate [2.5%, 97.5% CI]
Resistant-2016	Ricker	a	0.366 [0.238, 0.508]
		b	0.16 [0.139, 0.2]
Susceptible-2016	Ricker	a	0.394 [0.315, 0.466]
		b	0.152 [0.145, 0.175]
Resistant-2017	Holling Type IV	a	0.049 [0.04, 0.057]
		b	50.364 [ND, ND]
		c	-13.35 [-13.353, -13.348]
Susceptible-2017	Holling Type IV	a	0.111 [0.099, 0.123]
		b	52.354 [ND, ND]
		c	-13.234 [-13.234, -13.234]

ND = Not Determined; confidence intervals could not be calculated by inverting the Hessian matrix.

Table B4. Results of model selection among non-linear models for transmission.

Genotype-Year	Model	AIC _c	ΔAIC _c	df
Resistant-2016	Logistic Growth	13.14	0	2
	Ricker	13.15	0.01	2
	Linear	13.16	0.01	2
	Michaelis-Menten	14.21	1.07	2
	Holling Type IV	18.74	5.59	3
Susceptible-2016	Ricker	14.34	0	2
	Logistic Growth	15.35	1.01	2
	Linear	15.4	1.06	2
	Michaelis-Menten	16	1.66	2
	Holling Type IV	19.4	5.06	3
Resistant-2017	Holling Type IV	16.95	0	3
	Linear	19.87	2.92	2
	Ricker	19.88	2.93	2
	Michaelis-Menten	20.06	3.11	2
	Logistic Growth	22.55	5.6	2
Susceptible-2017	Ricker	16.37	0	2
	Michaelis-Menten	16.97	0.6	2
	Linear	17.93	1.56	2
	Logistic Growth	18.05	1.68	2
	Holling Type IV	18.7	2.33	3

AIC_c = Aikake's Information Criterion corrected for small sample size

ΔAIC_c = Difference between lowest AIC_c score and a given score

df = degrees of freedom, also the number of parameters

Table B5. Parameter estimates and 95% confidence intervals from best models of transmission.

Genotype-Year	Model	Parameter	Estimate [2.5%, 97.5% CI]
Resistant-2016	Ricker	a	0.704 [0.291, 1.032]
		b	0.344 [0.27, 0.524]
Susceptible-2016	Ricker	a	0.399 [0.172, 0.575]
		b	0.196 [0.151, 0.294]
Resistant-2017	Holling Type IV	a	0.069 [ND, ND]
		b	62.221 [ND, ND]
		c	-14.517 [ND, ND]
Susceptible-2017	Ricker	a	0.07 [0.021, 0.189]
		b	0.111 [0.011, 0.238]

ND = Not Determined; confidence intervals could not be calculated by inverting the Hessian matrix.

Supplementary Material. Appendix C. Secondary metabolites of *PdR1* resistant and susceptible grapevines

Sampling methods

We measured a profile of secondary metabolites from inoculated source plants within our transmission experiment. At the end of each trial, we collected two leaf blades and a 3 cm section of woody stem from each *X. fastidiosa*-infected source plant. We collected samples only from genotypes 092 Susceptible and 094 Resistant for logistical reasons.

Principal Components Analysis

To describe how secondary metabolites over the course of disease in the Resistant and Susceptible genotypes, we conducted a principal components (PC) analysis at each time point post-inoculation on the 105 individual secondary metabolites identified. We then tested which principal components clearly differed between genotypes using one-way ANOVAs, using the loadings of each PC for each observation. The approach is similar to principal components regression (e.g., Pareja et al. 2009) in that we sought to identify which set of secondary metabolites were most different between genotypes at each time point post-inoculation. However, here genotype (Resistant vs. Susceptible) was the sole explanatory variable and each PC was the response variable in a separate ANOVA. Following Pareja et al. (2009), we included only PCs that explained a cumulative 99% of total variance.

Ninety-nine percent of total variance in secondary metabolites was explained by the first six PCs at 2-weeks post-inoculation, 12 PCs at 5 weeks post-inoculation, 14 PCs at 8 weeks, and 11 PCs at 14 weeks. In each case these PCs were tested for differences between the two genotypes. Figure C1 plots the two most relevant PCs for each time point. At two weeks post-inoculation, we found no clear statistically significant difference between genotypes among any of the PCs tested. At five weeks post-inoculation, genotypes were clearly separated along PC2 ($F_{1,12} = 6.82$, $P = 0.023$) while they were less clearly different along PC7 ($F_{1,12} = 4.21$, $P = 0.063$). At eight weeks post-inoculation, genotypes strongly differed along PC4 ($F_{1,14} = 17.75$, $P < 0.001$) with loadings being overall lower in Resistant than Susceptible source plants (Fig. C1). Further examination of our PCA results suggest that, at eight weeks, the Resistant grapevines had relatively lower concentrations of compounds including quercetin, astragalín, kaempferol-7-O-glucoside, and kaempferol-3-O-glucoside; whereas these Resistant vines had greater concentrations of procyanidin- β -gallate 2, epicatechin gallate, and coumaric acid 1. At 14 weeks post-inoculation, genotypes were clearly separated to similar degrees along PC1 ($F_{1,11} = 6.35$, $P = 0.029$) and PC2 ($F_{1,11} = 6.64$, $P = 0.026$). The Resistant grapevines had relatively lower concentrations of compounds including astragalín, coumaric acid dimer, and kaempferol-7-O-glucoside, whereas Resistant vines had greater concentrations of Δ -viniferin, quercetin-3-O-glucoside in stems, epicatechin gallate, miyabenol C, piceid, unidentified volatile S, trans- and cis- β -ocimene, and coumaric acid 1.

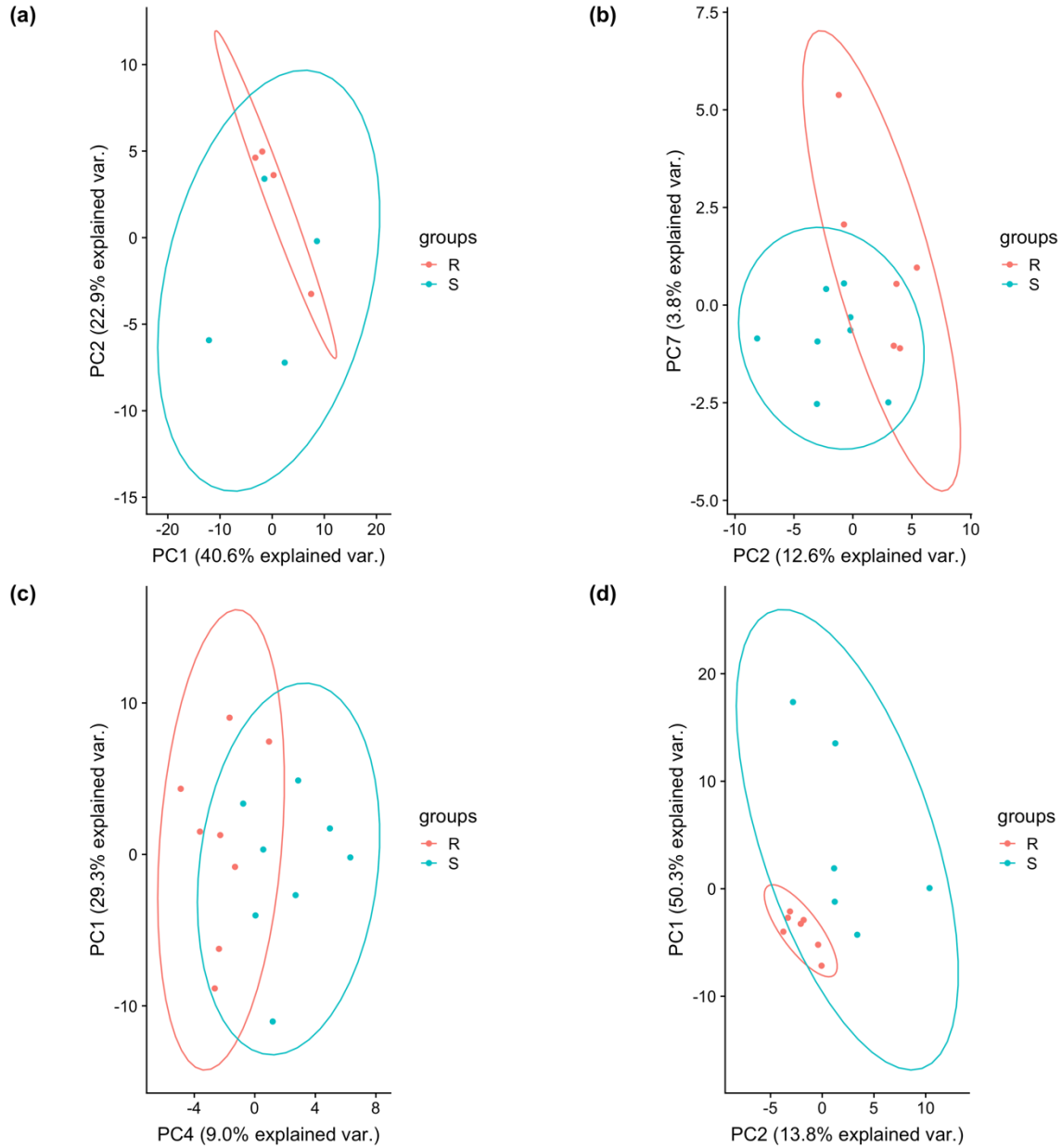


Figure C1. The Principal Components (PCs) that differed most between Resistant and Susceptible genotypes for all 105 secondary metabolites isolated from source plants at each time point: (a) 2 weeks, (b) 5 weeks, (c) 8 weeks, (d) 14 weeks post-inoculation. Individual points (i.e., source plants) are colored according to resistance status: orange = Resistance, blue = Susceptible. When fewer than two PCs were significantly different between genotypes, PC1 and PC2 are plotted. The percent of overall variation in the data set captured by each principal component is provided on the relevant axes.

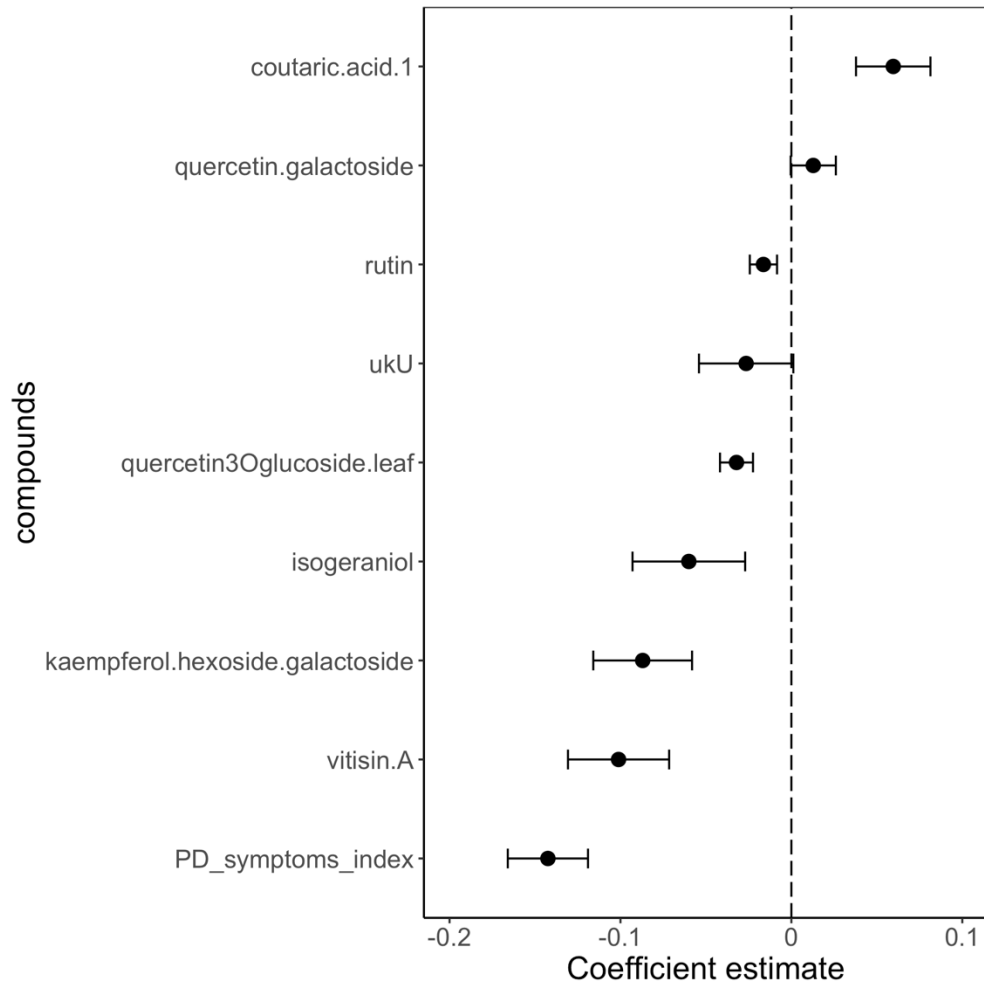


Figure C2. Mean coefficient estimates \pm SD from elastic net analysis of the relationship between secondary metabolite concentration (as well as PD symptom severity), on the y-axis, and estimated attraction rates for *G. atropunctata* vectors from the Consumer Movement Model to source plants. Negative coefficient estimates indicate that the predictor (i.e., compound) is negatively related to attraction rates. Means and standard deviations were calculated from 500 cross-validation runs. The most frequently selected values for the tuning parameters from cross-validation were $\alpha = 0.1$ and $\lambda = 1.55$. We excluded compounds that were dropped from the model (i.e., those that had a coefficient estimate of zero) in at least half of the cross-validation runs.

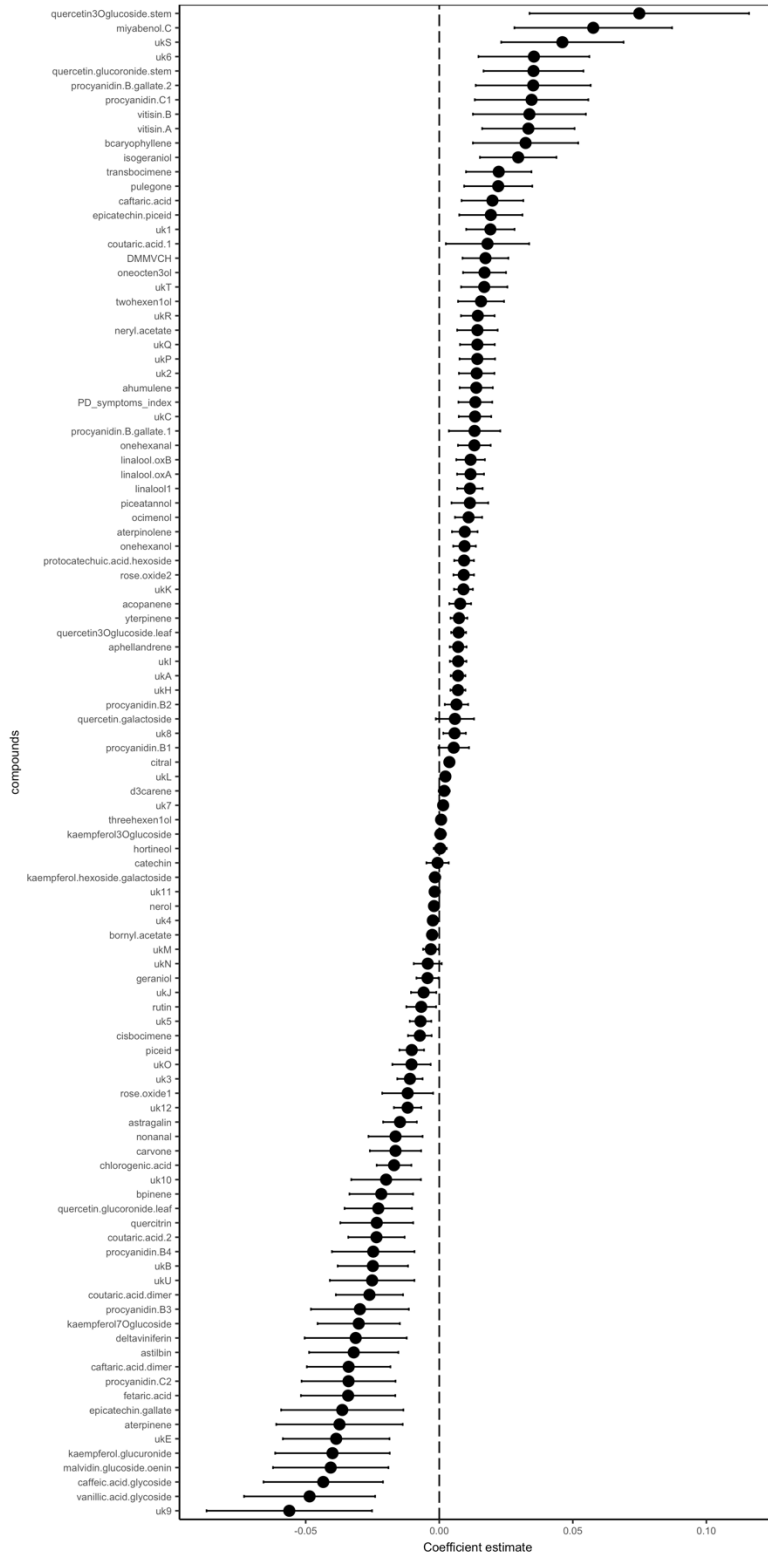


Figure C3. Mean coefficient estimates \pm SD from elastic net analysis of the relationship between secondary metabolite concentration (as well as PD symptom severity), on the y-axis, and estimated leaving rates for *G. atropunctata* vectors from the Consumer Movement Model from source plants. Negative coefficient estimates indicate that the predictor (i.e., compound) is negatively related to leaving

rates. Means and standard deviations were calculated from 500 cross-validation runs. The most frequently selected values for the tuning parameters from cross-validation were $\alpha = 0$ and $\lambda = 34.53$. No compounds were dropped from the model.

Supplementary Material Figure S1. Complete reinfection timeseries

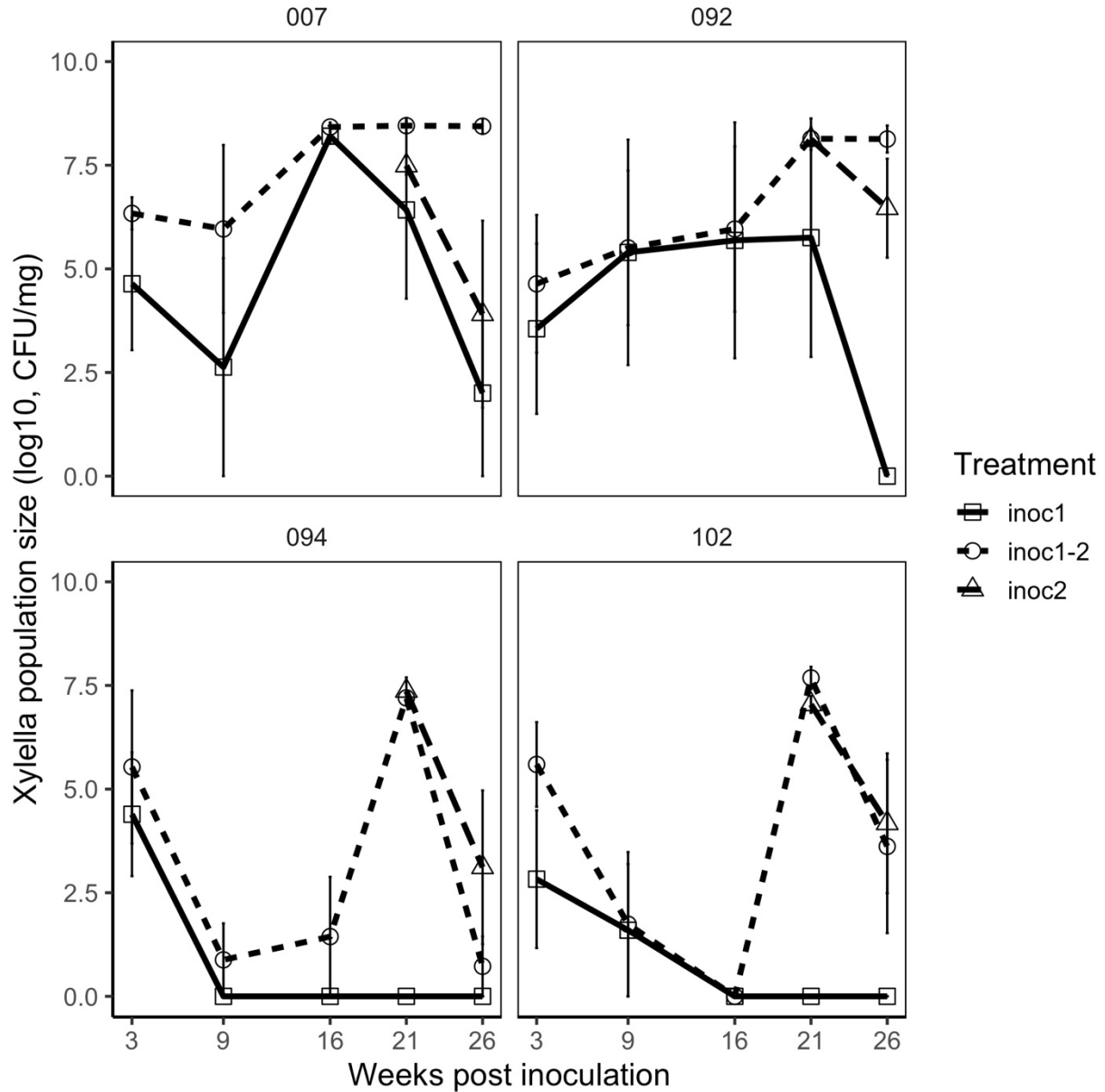


Figure S1. Complete timeseries for *X. fastidiosa* population size estimates from the reinfection experiment, measured over weeks since the first inoculation. Treatments include “inoc1” where plants were inoculated only at the first inoculation date; “inoc2” where plants were inoculated only at the second inoculation date; and “inoc1-2” where plants were inoculated at both inoculation dates. Second inoculation occurred 17 weeks after the first inoculation. Panels represent the different genotypes used in the experiment with Susceptible genotypes on the top row (007 and 092) and Resistant genotypes on the bottom row (094 and 102).

Literature Cited

- Adrakey HK, Streftaris G, Cunniffe NJ, et al (2017) Evidence-based controls for epidemics using spatio-temporal stochastic models in a Bayesian framework. *Journal of The Royal Society Interface* 14:20170386. doi: 10.1098/rsif.2017.0386
- Best A, White A, Boots M (2008) Maintenance of host variation in tolerance to pathogens and parasites. *PNAS* 105:20786–20791. doi: 10.1073/pnas.0809558105
- Blua MJ, Perring TM (1992) Effects of Zucchini Yellow Mosaic Virus on Colonization and Feeding Behavior of *Aphis gossypii* (Homoptera: Aphididae) Alatae. *Environ Entomol* 21:578–585. doi: 10.1093/ee/21.3.578
- Bolker B, R Core Team (2017) *bbmle: Tools for general maximum likelihood estimation* Bolker BM (2008) *Ecological Models and Data in R*. Princeton University Press, Princeton, NJ
- Boots M (2008) Fight or learn to live with the consequences? *Trends in ecology & evolution* 23:248–250
- Borer ET, Laine A-L, Seabloom EW (2016) A multiscale approach to plant disease using the metacommunity concept. *Annual Review of Phytopathology* 54:397–418. doi: 10.1146/annurev-phyto-080615-095959
- Burnham KP, Anderson DR, Huyvaert KP (2011) AIC model selection and multimodel inference in behavioral ecology: some background, observations, and comparisons. *Behav Ecol Sociobiol* 65:23–35
- Daugherty MP, Almeida RPP (2019) Understanding How an Invasive Vector Drives Pierce’s Disease Epidemics: Seasonality and Vine-to-Vine Spread. *Phytopathology* 109:277–285. doi: 10.1094/PHYTO-07-18-0217-FI
- Daugherty MP, Bosco D, Almeida RPP (2009) Temperature mediates vector transmission efficiency: inoculum supply and plant infection dynamics. *Annals of Applied Biology* 155:361–369. doi: 10.1111/j.1744-7348.2009.00346.x
- Daugherty MP, O’Neill S, Byrne F, Zeilinger A (2015) Is vector control sufficient to limit pathogen spread in vineyards? *Environmental Entomology* 44:789–797. doi: 10.1093/ee/nvv046
- Daugherty MP, Rashed A, Almeida RPP, Perring TM (2011) Vector preference for hosts differing in infection status: sharpshooter movement and *Xylella fastidiosa* transmission. *Ecol Entomol* 36:654–662. doi: 10.1111/j.1365-2311.2011.01309.x
- Daugherty MP, Zeilinger AR, Almeida RPP (2017) Conflicting effects of climate and vector behavior on the spread of a plant pathogen. *Phytobiomes* 1:46–53. doi: 10.1094/PBIOMES-01-17-0004-R
- De Miranda MP, Villada ES, Lopes SA, et al (2013) Influence of citrus plants infected with *Xylella fastidiosa* on stylet penetration activities of *Bucephalagonia xanthophis* (Hemiptera: Cicadellidae). *Ann Entomol Soc Am* 106:610–618. doi:10.1603/AN12148
- De Moraes CM, Stanczyk NM, Betz HS, et al (2014) Malaria-induced changes in host odors enhance mosquito attraction. *PNAS* 111:11079–11084. doi: 10.1073/pnas.1405617111
- Del Cid C, Krugner R, Zeilinger AR, et al (2018) Plant Water Stress and Vector Feeding Preference Mediate Transmission Efficiency of a Plant Pathogen. *Environmental Entomology*. doi: 10.1093/ee/nvy136
- Donnelly R, Cunniffe NJ, Carr JP, Gilligan CA (2019) Pathogenic modification of plants enhances long-distance dispersal of non-persistently transmitted viruses to new hosts. *Ecology* 0:e02725. doi: 10.1002/ecy.2725
- Dwyer G, Elkinton JS, Buonaccorsi JP (1997) Host heterogeneity in susceptibility and disease dynamics: tests of a mathematical model. *Am Nat* 150:685–707
- EFSA Panel on Plant Health (2015) Scientific Opinion on the risks to plant health posed by *Xylella fastidiosa* in the EU territory, with the identification and evaluation of risk reduction options. *EFSA Journal* 13:3989. doi: 10.2903/j.efsa.2015.3989
- Eigenbrode SD, Bosque-Pérez NA, Davis TS (2018) Insect-Borne Plant Pathogens and Their Vectors: Ecology, Evolution, and Complex Interactions. *Annu Rev Entomol* 63:169–191. doi: 10.1146/annurev-ento-020117-043119

- Feil H, Feil WS, Purcell AH (2003) Effects of date of inoculation on the within-plant movement of *Xylella fastidiosa* and persistence of Pierce's disease within field grapevines. *Phytopathol* 93:244–251. doi: 10.1094/PHYTO.2003.93.2.244
- Friedman J, Hastie T, Tibshirani R (2010) Regularization paths for generalized linear models via coordinate descent. *Journal of statistical software* 33:1
- Fritschi FB, Lin H, Walker MA (2007) *Xylella fastidiosa* Population Dynamics in Grapevine Genotypes Differing in Susceptibility to Pierce's Disease. *Am J Enol Vitic* 58:326–332
- Gandon S (2018) Evolution and manipulation of vector host choice. *The American Naturalist* 192:000–000
- Gilligan CA (2008) Sustainable agriculture and plant diseases: an epidemiological perspective. *Philosophical Transactions: Biological Sciences* 363:741–759
- Guilhabert MR, Kirkpatrick BC (2005) Identification of *Xylella fastidiosa* antivirulence genes: hemagglutinin adhesins contribute to *X. fastidiosa* biofilm maturation and colonization and attenuate virulence. *Molecular plant-microbe interactions* 18:856–868
- Harrell F (2019) *rms: Regression Modeling Strategies* Harrell FE (2015) *Regression Modeling Strategies*. Springer International Publishing, Cham
- Hill BL, Purcell AH (1997) Populations of *Xylella fastidiosa* in plants required for transmission by an efficient vector. *Phytopathology* 87:1197–1201. doi: 10.1094/PHYTO.1997.87.12.1197
- Hill BL, Purcell AH (1995) Acquisition and retention of *Xylella fastidiosa* by an efficient vector, *Graphocephala atropunctata*. *Phytopathology* 85:209–212
- James G, Witten D, Hastie T, Tibshirani R (2013) *An introduction to statistical learning*. Springer
- Jennersten O (1988) Insect Dispersal of Fungal Disease: Effects of *Ustilago* Infection on Pollinator Attraction in *Viscaria vulgaris*. *Oikos* 51:163–170. doi: 10.2307/3565638
- Johnson CR, Field CA (1993) Using fixed-effects model multivariate analysis of variance in marine biology and ecology. *Oceanography and Marine Biology Annual Review* 31:177–221
- Kingsolver JG (1987) Mosquito host choice and the epidemiology of malaria. *Am Nat* 130:811–827
- Krivanek AF, Riaz S, Walker MA (2006) Identification and molecular mapping of PdR1, a primary resistance gene to Pierce's disease in *Vitis*. *Theor Appl Genet* 112:1125–1131. doi: 10.1007/s00122-006-0214-5
- Krivanek AF, Stevenson JF, Walker MA (2005) Development and comparison of symptom indices for quantifying grapevine resistance to Pierce's disease. *Phytopathol* 95:36–43. doi: 10.1094/PHYTO-95-0036
- Krivanek AF, Walker MA (2005) *Vitis* Resistance to Pierce's Disease Is Characterized by Differential *Xylella fastidiosa* Populations in Stems and Leaves. *Phytopathology* 95:44–52. doi: 10.1094/PHYTO-95-0044
- Kuhn M, Wing J, Weston S, et al (2018) *caret: Classification and Regression Training* Laine A-L, Burdon JJ, Dodds PN, Thrall PH (2011) Spatial variation in disease resistance: from molecules to metapopulations. *J Ecol* 99:96–112. doi: 10.1111/j.1365-2745.2010.01738.x
- Lloyd-Smith JO, Schreiber SJ, Kopp PE, Getz W (2005) Superspreading and the effect of individual variation on disease emergence. *Nature* 438:355–359
- Luvisi A, Aprile A, Sabella E, et al (2017) *Xylella fastidiosa* subsp. *pauca* (CoDiRO strain) infection in four olive (*Olea europaea* L.) cultivars: profile of phenolic compounds in leaves and progression of leaf scorch symptoms. *Phytopathologia Mediterranea* 56:259-273–273. doi: 10.14601/Phytopathol_Mediterr-20578
- Macpherson MF, Kleczkowski A, Healey JR, et al (2017) The effects of invasive pests and pathogens on strategies for forest diversification. *Ecological Modelling* 350:87–99
- Marucci RC, Lopes JRS, Vendramim JD, Corrente JE (2005) Influence of *Xylella fastidiosa* infection of citrus on host selection by leafhopper vectors. *Entomologia Experimentalis et Applicata* 117:95–103. doi: 10.1111/j.1570-7458.2005.00336.x
- McElhany P, Real LA, Power AG (1995) Vector preference and disease dynamics: a study of barley yellow dwarf virus. *Ecology* 76:444–457

- Miller MR, White A, Boots M (2006) The Evolution of Parasites in Response to Tolerance in Their Hosts: The Good, the Bad, and Apparent Commensalism. *Evolution* 60:945–956. doi: 10.1111/j.0014-3820.2006.tb01173.x
- Mundt CC (2002) Use of multiline cultivars and cultivar mixtures for disease management. *Annual Review of Phytopathology* 40:381–410
- Nash JC, Varadhan R (2011) Unifying optimization algorithms to aid software system users: optimx for R. *J Stat Software* 43:1–14
- Nault LR, Ammar E-D (1989) Leafhopper and planthopper transmission of plant viruses. *Annual review of entomology* 34:503–529
- Neri FM, Cook AR, Gibson GJ, et al (2014) Bayesian Analysis for Inference of an Emerging Epidemic: Citrus Canker in Urban Landscapes. *PLOS Computational Biology* 10:e1003587. doi: 10.1371/journal.pcbi.1003587
- Pareja M, Mohib A, Birkett MA, et al (2009) Multivariate statistics coupled to generalized linear models reveal complex use of chemical cues by a parasitoid. *Animal Behaviour* 77:901–909. doi: 10.1016/j.anbehav.2008.12.016
- Perring TM, Gruenhagen NM, Farrar CA (1999) Management of plant viral diseases through chemical control of insect vectors. *Annual Review of Entomology* 44:457–481. doi: 10.1146/annurev.ento.44.1.457
- Power AG (1990) Cropping Systems, Insect Movement, and the Spread of Insect- Transmitted Diseases in Crops. In: Gliessman SR (ed) *Agroecology: Researching the Ecological Basis for Sustainable Agriculture*. Springer New York, New York, NY, pp 47–69
- R Core Team (2019) *R: A Language and Environment for Statistical Computing*. R Foundation for Statistical Computing, Vienna, Austria
- Rashed A, Killiny N, Kwan J, Almeida RPP (2011) Background matching behaviour and pathogen acquisition: plant site preference does not predict the bacterial acquisition efficiency of vectors. *Arthro-Plant Interact* 5:97–106. doi: 10.1007/s11829-010-9118-z
- Riaz S, Huerta-Acosta K, Tenschler AC, Walker MA (2018) Genetic characterization of *Vitis* germplasm collected from the southwestern US and Mexico to expedite Pierce’s disease-resistance breeding. *Theoretical and Applied Genetics* 1–14
- Roosien BK, Gomulkiewicz R, Ingwell LL, et al (2013) Conditional Vector Preference Aids the Spread of Plant Pathogens: Results From a Model. *Environmental entomology* 42:1299–1308
- Roy BA, Kirchner JW (2000) Evolutionary dynamics of pathogen resistance and tolerance. *Evolution* 54:51–63
- Ruijter JM, Ramakers C, Hoogaars WMH, et al (2009) Amplification efficiency: linking baseline and bias in the analysis of quantitative PCR data. *Nucleic Acids Res* 37:e45–e57. doi: 10.1093/nar/gkp045
- Senthil-Kumar M, Mysore KS (2013) Nonhost Resistance Against Bacterial Pathogens: Retrospectives and Prospects. *Annual Review of Phytopathology* 51:407–427. doi:10.1146/annurev-phyto-082712-102319
- Shaw AK, Peace A, Power AG, Bosque-Pérez NA (2017) Vector population growth and condition-dependent movement drive the spread of plant pathogens. *Ecology* 98:2145–2157. doi: 10.1002/ecy.1907
- Shoemaker LG, Hayhurst E, Weiss□Lehman CP, et al (2019) Pathogens manipulate the preference of vectors, slowing disease spread in a multi-host system. *Ecology Letters* 0: doi: 10.1111/ele.13268
- Sicard A, Zeilinger AR, Vanhove M, et al (2018) *Xylella fastidiosa*: insights into an emerging plant pathogen. *Annual Review of Phytopathology* 56:1–22. doi: 10.1146/annurev- phyto-080417-045849
- Sisterson MS (2008) Effects of insect-vector preference for healthy or infected plants on pathogen spread: insights from a model. *J Econ Entomol* 101:1–8
- Sisterson MS, Stenger DC (2018) Modelling effects of vector acquisition threshold on disease progression in a perennial crop following deployment of a partially resistant variety. *Plant Pathology* 67:1388–1400. doi: 10.1111/ppa.12833

- Tumber K, Alston J, Fuller K (2014) Pierce's disease costs California \$104 million per year. *California Agriculture* 68:20–29
- Venables WN, Ripley BD (2002) *Modern Applied Statistics with S*, 4th edn. Springer, New York, NY
- Walker MA, Tenschler AC (2016) Breeding Pierce's disease resistant winegrapes. In: *Proceedings of the 2016 Pierce's Disease Research Symposium*. California Department of Food and Agriculture, San Diego, CA, pp 167–177
- Wallis CM, Chen J (2012) Grapevine Phenolic Compounds in Xylem Sap and Tissues Are Significantly Altered During Infection by *Xylella fastidiosa*. *Phytopathology* 102:816–826. doi: 10.1094/PHYTO-04-12-0074-R
- Wallis CM, Wallingford AK, Chen J (2013) Effects of cultivar, phenology, and *Xylella fastidiosa* infection on grapevine xylem sap and tissue phenolic content. *Physiological and Molecular Plant Pathology* 84:28–35. doi: 10.1016/j.pmpp.2013.06.005
- Watkinson-Powell B, Gilligan CA, Cunniffe NJ (2019) When does spatial diversification usefully maximise the durability of crop disease resistance? *bioRxiv* 540013. doi: 10.1101/540013
- Werner BJ, Mowry TM, Bosque-Pérez NA, et al (2009) Changes in Green Peach Aphid Responses to Potato Leafroll Virus—Induced Volatiles Emitted During Disease Progression. *Environmental Entomology* 38:1429–1438. doi:10.1603/022.038.0511
- Zeilinger AR, Daugherty MP (2014) Vector preference and host defense against infection interact to determine disease dynamics. *Oikos* 123:613–622. doi: 10.1111/j.1600-0706.2013.01074.x
- Zeilinger AR, Olson DM, Andow DA (2014) A likelihood-based biostatistical model for analyzing consumer movement in simultaneous choice experiments. *Environ Entomol* 43:977–988. doi: 10.1603/EN13287
- Zeilinger AR, Olson DM, Maclean D, et al (2015) Behavioural and chemical mechanisms of plant-mediated deterrence and attraction among frugivorous insects: Herbivore-induced deterrence and attraction. *Ecological Entomology* 40:532–542. doi:10.1111/een.12221
- Zou H, Hastie T (2005) Regularization and variable selection via the elastic net. *Journal of the Royal Statistical Society Series B (Methodological)* 67:301–320